Chapter 1

Introduction

1-1. Overview of polycrystalline silicon thin-film transistor technology

The first generation of active matrix liquid crystal displays (AMLCDs) used a-Si: H TFT as the pixel switching device. The main advantages of the a-Si:H TFT are the low process temperature that can avoid damaging the glass substrate and the low leakage current that can avoid grey level shift as the TFT is turned off. However, the low electron field effect mobility (typically below 1 $cm^2V^{-1}S^{-1}$) as these devices adopted on glass limits the capability of advanced and integrated circuit on the glass. Integration of driver circuitry with display panel on the same substrate is very desirable not only to reduce the module cost but to improve the system reliability.

Recently, polycrystalline silicon thin-film transistors (poly-Si TFTs) have attracted much attention because of their widely applications in active matrix liquid crystal displays (AMLCDs) and organic light-emitting diodes (OLEDs). Comparing with a-Si:H TFTs, poly-Si TFTs can provide higher electron mobility (by two orders of magnitude) and higher driving current allowing smaller TFT size to be used as the pixel-switching elements, resulting in higher aperture ratio and lower parasitic gate-line capacitance for improved display performance. In addition to flat panel displays, poly-Si TFTs have also been applied into some memory devices such as dynamic random access memories (DRAMs), static random access memories (SRAMs), electrical programming read only memories (EPROM), and electrical erasable programming read only memories (EEPROMs). Among the poly-Si technologies, low temperature polycrystalline silicon thin-film transistors (LTPS TFTs)

are primarily applied on glass substrates since higher process temperature may cause the substrate bent and twisted. Up to now, dozens of researches have been made to develop various technologies for improving the performance and reliability of LTPS TFTs. Since the electron field-effect mobility of LTPS TFTs is larger than a-Si: H TFTs but smaller than MOS transistors, it is anticipated that matured poly-si technology may realize the so-called "System on Glass, SOG" technology, which will be introduced in the next section.

1-2 The capability for LTPS TFTs to realize System on Glass, SOG

In AMLCDs, each gate line and data line is addressed by peripheral circuits. In nowadays LCDs, the peripheral circuits are composed of many LSI driving circuits and connected to the panel through print circuit boards (PCB). This causes two problems as the display resolution increases. First, assembly becomes more complicated because the place around the panel is needed for many LSI circuits and printed board, while the space available in AMLCDs is usually limited. Second, the usage of peripheral circuits and the assembly processes are usually so much that the reduction of manufacturing cost is inhibited. Besides, as the resolution increases, the pin number on the PCB will accordingly increases, which will as well lead to the yield decrease during process.

The idea of system on glass comes from the integration of circuits onto the glass with panels. Since LTPS TFTs can provide the electron field effect mobility over 50 $cm^2V^{-1}s^{-1}$, some peripheral circuits used in AMLCD can adopt these TFTs as the transistors and be integrated on glass. In addition to cost reduction, integration of peripheral circuits can also decrease the module weight and increase panel reliability.

In many works, poly-si TFTs have demonstrated a great advantage over those built in a-Si ones even in large size active matrix displays with the peripheral circuit integrated on the same substrate. With advanced poly-si technology and higher electron mobility in poly-si TFTs in the future, it can be estimated that the peripheral circuit would be fully integrated on glass and the perspective of "system on glass" could be realized.

1-3 Device variation

LTPS TFTs are found to suffer serious behavior variation. Devices from predominant process condition still exhibit electrical behavior variation. Though the device structure is similar to MOSFETs (Metal-Oxide-Silicon Field Effect Transistors), the variation behaviors of TFTs are much worse than those of MOSFETs. Since the variation of device behavior may directly affect the circuit performance and reliability prediction, it would be very essential to have a clear understanding of how the variation may come and the behaviors the variation could be. Before investigating the variation behavior in LTPS TFT, we would review the study of variation in IC.

The variation issue studied in designing ICs is called the mismatch between identically designed devices. It constitutes a serious limiting factor of the accuracy of analog integrated circuits such as digital-to-analog converters and sense amplifiers for memory arrays. Mismatch is the effect that causes a dependence of correlation between parameters of identical devices on their mutual distance, so that equally designed devices display different statistical behaviors. This dependence is due to the nonuniformity of process parameters, considered as the source of statistical variations of the die, so that they must be related to the mutual distance of the die.

Mismatch sources can be divided as local variations characterized by short

correlation distances and global variations characterized by long correlation distances, where the correlation distance is defined as the distance in which a process disturbance affects the device performances. If this distance is lower than the usual distance between devices, the disturbance constitutes a local variation and affects at most one device (e.g. a charge trapped in the gate oxide layer). On the other hand, the global variation, characterized by process disturbances with longer correlation distances (e.g. the gate oxide thickness across the wafer surface), affects all the devices within a defined region. Therefore the relative positions of the devices determine the effect of global variations on parameter mismatch. In other words, devices placed at large distance are more affected by global variations than devices placed close to each other.

In IC, the global variations are further extended as wafer-to-wafer, batch-to-batch and lot-to-lot variation. The variation issue is examined with respect to the mutual device distance. In the application using MOSFETs with high sensitivity to the mismatch variations such as current mirrors, digital-to-analog converters, and sense amplifiers, the statistical variation analysis would be a very important verification step. In the scope of this thesis, since the LTPS TFTs may be used to make advanced circuitry and the perspective of SOG, the uniformity issue would become more essential. Owing to the low process temperature, LTPS TFTs have different process from IC industry. This may be the source of device behavior variation. Besides, LTPS TFTs have less controllable defect number and distribution in the poly-silicon film. In our work, we classify the variation as macro variation and micro variation. Macro variation comes the issues of process control, such as gate insulator thickness, LDD length fluctuation and ion implantation uniformity. This non-uniformity of process control will result in the common shift of device parameters. On the other hand, micro variation comes from the difference of the defect site, defect density in the active

region and the activation efficiency. Since these conditions vary from device to device, micro variation will lead to the random distribution of device parameter. In chapter 2, the uniformity issue of LTPS TFTs will be discussed with respect to mutual device distance.

1-4 Motivation

Up to now, very few researches have been made on the variation issue of LTPS TFTs. Most researches about LTPS TFTs aim at the improvement of the device performance. However, before LTPS TFTs can be widely-applied in mass production, the study of device variation is crucial and necessary. In this thesis, we focus the variation behavior of LTPS TFTs and its influences on device reliability and circuit.

In chapter 2, we start from examining the variation behavior of LTPS TFTs on different glasses. In order to distinguish the influence of macro and micro variation, we propose a new device layout, e.g. the crosstie layout. By using this layout, the effects of macro and micro variation are separated and quantitatively studied. Since the TFTs used in flat panel displays are usually operated in high voltage, the reliability of TFTs is essential. In chapter 3, we investigate the device reliability affected by device variation. Because LTPS TFTs are capable of advanced circuitry and peripheral circuit, the relation between device variation and circuit performance should as well be studied. In chapter 4, we use a simple and widely-used circuit, source follower, to examine the circuit performance influenced by device variation.

1-5 Thesis Outline

Chapter 1-Introduction

1-1 Overview of poly-si TFTs

1-2 The capability for LTPS TFTs to realize SOG

1-3 Device variation

1-4 Motivation

1-5 Thesis outline

Chapter 2-The variation of LTPS TFTs

2-1 Parameter extraction and analysis method

2-1-1 Typical device parameters

2-1-2 Statistical analysis method

2-2 Glass-to-glass uniformity

2-3 Device-to-device uniformity

2-4 Summaries

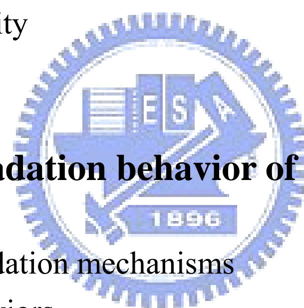

Chapter 3-Diverse degradation behavior of LTPS TFTs with device variation

3-1 Introduction to two degradation mechanisms

3-2 Diverse degradation behaviors

3-3 Discussion of the degradation behavior and device variation

Chapter 4- Circuit performance of LTPS TFTs with device variation

4-1 Introduction to source follower

4-2 The special charging behavior

4-3 Discussion of the charging behavior and device variation

Chapter 5- Conclusions

References

Figures

Chapter 2.

Spatial Uniformity

2-1 Parameter extraction and analysis method

In this section, we introduce the extraction methods for typical parameters of the TFTs and the statistical approaches to analyze the distribution of these parameters in this thesis. Threshold voltage Vth, electron mobility Mu and subthreshold swing S.S. are chosen to be analyzed since these three important indices are the typical and important parameters to describe the turn-on behavior of devices. To examine the distribution and the deviation from normal distribution, we adopt the histogram, the Q-Q plot (quantile–quantile plots) and the detrended Q-Q plots, which will be explained in the following.

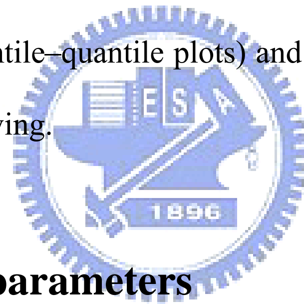

2-1-1 Typical device parameters

Plenty methods are used to determine the threshold voltage, which may be the most important parameter in application. In most of the researches on TFT, the constant current method is widely-adopted. In this thesis the threshold voltage is determined from this method, which extracts Vth from the gate voltage at the normalized drain current Id=10nA for Vd=0.1V.

Subthreshold swing S.S (V/dec) is a typical parameter to describe the control ability of gate toward channel. The subthreshold swing should be independent of drain voltage and gate voltage. However, in reality, the subthreshold swing might increase with drain voltage due to short-channel effects. It might as well be affected by the serial resistance and interface traps and therefore become related to the gate

voltage. In this work, it is defined as the minimum of the gate voltage required to increase drain current by one order of magnitude.

The electron field effect mobility Mu is determined from the transconductance g_m at low drain voltage. The transfer characteristics of poly-si TFTs are similar to those of conventional MOSFETs, so the first order I-V relation in the bulk Si MOSFETs can be applied to the poly-Si TFTs, which can be expressed as

$$I_D = \mu_{FE} C_{ox} \frac{W}{L}[(V_G - V_{TH})V_D - \frac{1}{2}V_D^{\ 2}] \qquad (2\text{-}1)$$

Where

C_{ox} is the gate oxide capacitance per unit area,

W is channel width,

L is channel length,

V_{TH} is the threshold voltage.

If the drain voltage Vd is much smaller compared with $V_G - V_{TH}$, then the drain current can be approximated as:

$$I_D = \mu_{FE} C_{ox} \frac{W}{L}(V_G - V_{TH})V_D. \qquad (2\text{-}2)$$

And therefore the electron field effect mobility can be expressed as:

$$\mu_{FE} = \frac{L}{C_{ox} W V_D} g_m \qquad (2\text{-}3)$$

Where the transconductance is defined as:

$$g_m = \frac{\partial I_D}{\partial V_G}\Big|_{V_D = const.} = \frac{W C_{ox} \mu_{FE}}{L} V_D \qquad (2\text{-}4)$$

2-1-2 Statistical analysis method

In statistics the standard deviation value, σ, is usually used to investigate the distribution of the observed value. The standard deviation value is given as

$$\sigma \equiv \sqrt{\frac{1}{n}\sum_{n}(\chi-\overline{\chi})^{2}} \quad \text{Where } \chi \text{ is the observe value} \qquad (2\text{-}5)$$

This parameter represents the difference between the observed values and the corresponding mean value. In a normal distribution, 99.7% of the total observed samples will fall in the region three times of σ from the average value. In other words, three times of the deviation value will provide the information how broad this distribution may be. If σ is large, it means that the value of the observed samples will fall in a large range and result in the broad distribution in the histogram. By simply adding the average value and three times of the deviation value, we can realize the range that most of the observed values actually fall in, even the distribution is not a Gaussian distribution.

In order to examine the distribution of measured data and the deviation from the normal distribution, we adopt the histogram, the Q-Q plot (quantile–quantile plots) and the detrend Q-Q plot. The histogram is the most common graph to examine the distribution of an observed value. A histogram is a rectangular graph of a frequency distribution. To test the normality of the distribution, the graphical methods include the use of probability plots are developed. These can be either P-P plots (probability–probability plots), in which the empirical probabilities are plotted against the theoretical probabilities for the distribution, or Q-Q plots (quantile–quantile plots), in which the sample points are plotted against the theoretical quantiles. The Q-Q plots are more common because they are invariant to differences in scale and location. If the assumed population is correct, then the observed value and the expected value for each case would be very close to each other. If the observations come from a specific distribution, then the plotted points should roughly lie on a straight line. On the other hand, if the assumed population is not correct, then the observed and expected value would not be approximately the same and the points in this plot would not follow the

45° straight line. Thus, if the points in this plot are close to the line of identity, this plot supports the reasonableness of the assumed population distribution. For the same reason, if the plotted points deviate markedly from the line of identity, then the plots also provide evidence that the assumed distribution is not the appropriate model to describe the observed value. Especially for the normal distribution, the Q-Q plots are known as the normal probability plots, which are adopted in this thesis.

A residual is the difference between an observed value and the corresponding anticipated value. A graphic presentation of residuals, called a residual plot, is useful for highlighting major departures between the observed and the anticipated patterns or relationships in a data set. The detrend Q-Q plot is one of the residual analysis. The residual analysis refers to a set of diagnostic methods for investigating the appropriateness of a regression model utilizing the residuals. If a regression model is appropriate, the residuals should reflect the properties ascribed to the mode error terms ε_i. For instance, since regression model assumes that the ε_i are normal random variables with constant variance, the residuals should show a pattern consistent with these properties. If the model is appropriate, the residuals should reflect the properties ascribed to the model error terms. Using the normal probability plots of the residuals, where the ranked residuals are plotted against their expected values under normality, we may further investigate the difference between the distribution of the measured data and the normal distribution.

2-2 Glass-to-glass uniformity

In the following sections, we discuss the uniformity issue of LTPS TFTs with respect to the mutual device distance. The main purpose is to distinguish the source of device variation. We first start from the devices on different glasses.

The process flow of fabricating the LTPS TFTs in this work is described as follows. First, the buffer oxide and a-Si: H films were deposited on glass substrates, and then XeCl excimer laser was used to crystallize the a-Si: H film, followed by poly-Si active area definition. Subsequently, a gate insulator was deposited. Next, the metal gate formation and source/drain doping were performed. A lightly doped drain (LDD) structure was used on the devices. Dopant activation and hydrogenation were carried out after interlayer deposition. Finally, contact holes formation and metallization were performed to complete the fabrication work. The devices with channel width W = 20 μm and channel length L = 6 μm are used in this work and the I-V characteristics were measured by using an HP 4156 semiconductor parameter analyzer.

Fig. 2-2-1, 2-2-2 and 2-2-3 are the average and deviation values of the threshold voltage, electron mobility and subthreshold swing of specific device position on different glasses. The relative position of site A to H is defined in Fig.2-2-4. Table 2 is the values for these parameters. From Fig 2-2-1, it can be seen that the average value AVG of the Vth of these sites range from 0.96 to 1.29 V, while the standard deviation STD range from 0.33 to 0.52 V. The standard deviation of total devices and the deviation is about 0.446 V.

Refer to the table, it can be seen that the deviation values of these eight locations are similar, which means the broadness of the Vth of these sites are similar. If the variation mainly comes from one particular step in the process, then the variation may exhibit steep increase in the specific site. Take deposition process for example, if the variation comes from the uniformity of film deposition of PECVD (Plasma-Enhanced Chemical Vapor Deposition), then the uniformity may show large difference between the central region and the outer region. In this work it should correspondingly exhibit differences between site C, D, E, F and site A, B, G, H. Since

this is not observed in our data, we may infer that the variation of these devices do not result from the single process step. However, because these data come from the devices on different glasses, this variation of device parameter actually includes macro and micro variation. In order to investigate the relation between device behavior variation and macro/micro variation, we further examine the device behavior variation using our proposed layout.

AVG		Vth (V)	Swing(V/dec)	Mobility(cm^2/VS)
	SiteA	1.2738	0.26288	69.3701
	SiteB	1.22663	0.26443	78.4022
	SiteC	0.96174	0.29959	72.89819
	SiteD	1.29921	0.26395	76.43811
	SiteE	1.1486	0.28523	72.58952
	SiteF	1.28153	0.26909	75.05665
	SiteG	1.08431	0.26475	69.8103
	SiteH	1.03824	0.27091	76.87074
		Vth (V)	Swing(V/dec)	Mobility(cm^2/VS)
STD	SiteA	0.51688	0.05036	11.26466
	SiteB	0.34866	0.04519	12.30325
	SiteC	0.3638	0.04988	11.72347
	SiteD	0.52264	0.04266	12.57617
	SiteE	0.49769	0.04746	11.67293
	SiteF	0.46335	0.04856	12.24387
	SiteG	0.34728	0.05412	10.64023
	SiteH	0.33401	0.0403	11.08413

Table 2 The mean value and the standard deviation value of the devices in

different sites.

2-3 Device-to-device uniformity

Intuitively, if devices can be fabricated very close to each other, the process condition will be almost the same and macro variation can therefore be ignored. However, owing to the margin of process step such as photo-mask alignment and etching, the distance between devices can not be infinitely close and in practical the distance is about several decades of micrometers. In this work we used a special layout to investigate the relationship between uniformity issue and device distance. In the following section we denote the distance between two devices by the distance of the polysilicon film.

Fig 2-3-1 is the layout of the devices we adopted in this section. The red, blue and yellow regions respectively represent the polysilicon film, the gate metal and the source/drain metal. The structure of the poly-si film and the gate metal are in the order that resembles the crosstie of the railroad and therefore this layout is called the crosstie type layout of LTPS TFTs. The distance of two nearest active regions is equally-spaced 35 μm. In this small distance the macro variation may be ignored, and the variation of device behavior can therefore be reduced to only micro variation.

Fig 2-3-2 to 2-3-10 are the Vth, mobility and subthreshold swing of the crosstie type TFTs and the corresponding Q-Q plot and the detrended Q-Q plot. It can be seen that Vth and swing comprise similar distribution of normal distribution. Refer to the Q-Q plot and the detrended Q-Q plot, the observed values and the fitting normal distribution values are both very close. This distribution of Vth and swing meet our expectation since from the viewpoint of statistic process control, the device parameter should exhibit normal distribution under well-controlled process condition.

The Vth variation of devices with different device distances is shown respectively from Fig 2-3-11 to Fig 2-3-17. The distance of the devices is numbered with the unit “step”, which denotes the space between two nearest devices. It can be seen that the variability of the devices is following normal distribution as the distance between devices is one step, which is only 35 μm on mask. In this small dimension, the variation can be totally attributed to micro variation. As the mutual device distance increases, it can be seen that the distribution of device variability is gradually distorted and the center is gradually shifting positive. As for the device distance is small, the distribution is approximately following Gaussian distribution. As the distance increases, the distribution of Vth difference is gradually flattened and distorted away from Gaussian.

Fig 2-3-18 is the Vth value of the crosstie devices of the different positions on the glass. The red rectangular is the mean value of the Vth of the devices in the local region. These red triangles show that the average value of the threshold voltages exhibit the threshold voltage shift aggregatively. This common shift corresponds to the macro variation. Besides, it can be seen that in the local region the Vth value will exhibit random variation, which corresponds to micro variation. The deviation value of these three regions is almost the same, indicating that the micro variation causes similar effect on these devices. Compared with Fig 2-2-1, it can be seen that the effect of micro variation is about one-twentieth of the total variation.

In order to examine the relationship between variation behavior and device distance, we statistically sort the Vth difference of a specific device distance. Fig 2-3-19 is the average and deviation value of Vth difference with respect to different device distance. The black solid rectangular denotes the average value of the Vth difference of the devices of a specific device distance, while the empty blue triangle denotes the standard deviation of the Vth difference. It can be seen that the average

value of the Vth difference of the devices increases as the device distance increases, which corresponds to the macro variation. This reveals that the macro variation depends on device distance and as the device distance increases, macro variation may gradually dominate the variation of device parameters.

It can also be seen that the deviation of Vth difference is almost independent of device distance. As the mutual device distance increases, this deviation is not changing and the value is around 0.03V. We now adopt a formula in statistics to explain this characteristic. If two distributions X and Y with random variable and respectively the deviation of the distribution $\sigma\{X\}$ and $\sigma\{Y\}$ are known. The variance of the difference of two dependent random variables X and Y are as follows:

$$\sigma^2\{X\text{-}Y\} = \sigma^2\{X\} + \sigma^2\{Y\} - 2\sigma\{X, Y\} \qquad (2\text{-}6)$$

where $\sigma\{X, Y\}$ is the covariance of two continuous random variables and $\sigma\{X\}$ and $\sigma\{Y\}$ are the standard deviations of X and Y.

The covariance of two discrete random variables is defined:

$$\sigma\{X, Y\} = \Sigma\Sigma(x - E\{X\})(y - E\{Y\})\ P(x,y) \qquad (2\text{-}7)$$

P(x, y) denotes the relation of X and Y. If X and Y are independent, P(x, y) =0 and therefore $\sigma\{X, Y\} = 0$. When $\sigma\{X, Y\}$ is positive, we say that X and Y exhibit positive covariance. When $\sigma\{X, Y\}$ is negative or zero, we say that X and Y exhibit negative or zero covariance. In our case, the covariance corresponds to the relationship of the devices from two local regions on the glass. Since these devices are identical, these devices are independent and the covariance should be zero. Therefore, the variance of the differences of the devices from two regions should only relate to the standard deviation of the two regions. Refer to Fig 2-3-18, the standard deviation of the local devices is both about 0.02V and by using the relation (2-6), the variance of the difference of the devices from two regions can be calculated that $\sigma\{X\text{-}Y\}$ is approximately 0.03V, which is the same from Fig 3-3-19. This invariant variance of

Vth difference reveals that micro variation does not vary as device distance increases and is independent of device distance. In other words, Fig 3-3-19 indicates that macro variation changes is dependent of device distance, while micro variation is independent of device distance. Since the sources of macro and micro variation are different, it can be expected that the variation may be suppressed respectively.

2-4 Summaries

In this chapter, the uniformity issue is investigated with respect to device distance. We first examine the devices from different glasses and find that the device parameters comprise wide distributions. Then, to decouple the macro variation and micro variation, we introduce the crosstie type layout of LTPS TFT, which the nearest devices are spaced only 35 μm and macro variation can therefore be ignored. It is found as the device distance increases, the difference of the threshold voltage indeed increases, and the distribution is gradually distorted from Gaussian distribution. We further found that the macro variation is dependent on the device distance and varies with device distance. On the other hand, by referring to the formula from Statistics, it can be inferred that micro variation is independent of device distance. Since the variation is classified and quantified, it can be expected that the variation may be depressed.

Chapter 3
Diverse degradation behavior of LTPS TFTs with device behavior variation

There are many researches reported about the reliability issue of LTPS TFTs under different stress conditions. The degradation phenomena[1~7] are caused by factors such as hot carrier effect, thermal effect, water, contamination and electrostatic discharge (ESD). In chapter 2, it is demonstrated that LTPS TFTs suffer from serious device variation. In this section, we focus on the reliability issue of large stress drain voltage with device behavior variation.

3-1 Introduction to the degradation mechanism for devices under large drain voltage

1896

As large drain voltage is applied to the TFT, high lateral electric field is induced in the device and many degradation mechanisms may occur, in particular hot carrier effect and thermal effect. As large drain voltage is applied and the gate voltage is not large, the induced carriers will gain very high kinetic energy after being accelerated by a strong electric field in areas of high field intensities within the device and can get injected and trapped in areas of the device where they should not be, forming a space charge that causes the device degrade or become unstable. In poly-Si, since the number of trap is larger, the hot carrier effect is accordingly worse.

On the other hand, as the gate voltage increases and correspondingly the equivalent lateral electrical field decreases, the hot carrier effect is reduced. Instead, the power in the device is becoming high, causing the temperature of TFTs increased due to Joule heat, which is known as self-heating or thermal effect. Since TFTs are

fabricated on glass substrate, the heat dissipation to the substrate is relatively low and makes the degradation worse.

3-2 Diverse degradation behaviors of LTPS TFT with electrical characteristic variation

Fig. 3-2-1 shows a typical Id-Vg curves of the TFT undergoing thermal effect, while Fig. 3-2-2 shows the transfer characteristics of the device experiencing hot carrier effect. In thermal effect case, the subthreshold region and the threshold voltage are serious degraded. For the changes in the transfer behaviors of hot carrier effect, the drain current is degraded in the saturation region and almost unchanged in the subthreshold region. Therefore these two degradation mechanism may be distinguished by the subthreshold swing difference after stress. As shown in Fig.3-2-3, in examining the swing degradation with respect to different stress gate voltage Vg with Vd kept at 20V, it is observed that the swing degradation shows steep increase near Vg=12V~ 14V, where the swing degradation is defined as the swing difference before and after stress. It was reported[8] that there are regions these two degradation mechanism separately dominate and for devices with W/L= 100 μm/10 μm, the boundary of these two mechanism at Vd=20V is approximately Vg=12.5V. It was also reported[9] that the mobility degradation ratio suffers from serious degradation variation under this boundary stress condition. Therefore, it would be essential to examine the degradation behaviors under this stress condition with device characteristic variation. Hence several devices with different Vth are stressed under the stress condition Vd=20V and Vg=12~13 V and time duration 500s, and the degradation behaviors are shown in Fig.3-2-4 with solid dots. It can be seen that large variation of swing degradation is observed in this region. The transfer characteristics and degradation behaviors of devices A and B with larger swing degradation are

shown in Fig. 3-2-5 and devices X and Y with smaller swing degradation as well as a particular device are shown in Fig. 3-2-6 and 3-2-7. In Fig. 3-2-5, as for devices having small Vth their Id-Vg curves exhibit serious degradation in the subthreshold region and saturation region. It is shown that both Vth and subthreshold swing are greatly increased, and mobility is decreased, which indicates that these devices suffer from degradation of thermal effect. On the contrary, refer to Fig. 3-2-6, devices having large Vths do not exhibit this degradation mechanism. It can be seen that the transfer characteristics of devices X and Y are slightly shifted in the negative direction while the saturation region also degraded. It is reported[10~11] that the threshold voltage shift may be caused by the mobile ions at the MOS interface in the n-channel TFTs during stress. Comparing Fig. 3-2-5 and Fig. 3-2-6, it reveals that under the same stress condition, devices with smaller Vth seem to suffer from thermal effect while devices with larger Vth seem to suffer from hot carrier effect.

We attribute this diverging phenomenon to the variation of the initial Vth of the devices. The degradation behaviors are replotted with respect to the stress gate voltage subtracts the initial Vth, i.e. Vg-Vth. Refer to Fig. 3-2-4, the empty dots denote the degradation behaviors of the devices and the arrows describe the initial Vth of these devices. It can be seen that smaller value of (Vg-Vth) leads to smaller swing degradation, while larger value leads to worse degradation behaviors. It can also be seen that under the same stress condition devices with smaller Vth shift less and fall in the upper region of the plot, while devices with larger Vth shift more and fall in the lower region of the plot. Therefore, it depicts that there is a boundary separating these two degradation behaviors by the value Vg-Vt instead of Vg. This is different from the expectation that devices under the same stress condition should exhibit similar degradation behavior.

Considering the negative Vth shift arisen by the mobile ions, it is expected that the

device degradation may sway between the hot carrier effect and thermal effect, and the device would exhibit two-step degradation behavior as stress time increases. To verify this assumption, several LTPS TFTs with different Vth under are stressed this special stress condition. Refer to Fig. 3-2-7, the specific device D with initial Vth=3.67 V is found to experience hot carrier effect with stress time of the first 100 seconds, and the Vth after stress is slightly shifted to 3.47 V. Then this device further exhibits thermal effect degradation as stress time increases, which can be identified by the gradually degraded subthreshold swing and threshold voltage in the curves of stress time 200 seconds and 500 seconds. It is obviously seen that this device actually experienced two kind of degradation mechanism under this critical stress condition as the stress time increased. This two-step degradation mechanism further verifies the existence of the boundary and we can consequently infer that this boundary separating these two degradations is as narrow as 0.2 V under this stress condition.

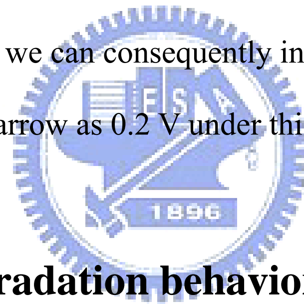

3-3 Discussion of degradation behavior and device variation

Conventionally devices under the same stress condition will exhibit similar degradation behavior. However, it is shown that the reliability of LTPS TFT is related to the variation of the devices. Under a critical stress condition, it is demonstrated that devices with different threshold voltage will exhibit different degradation behaviors. The boundary dividing these two degradation behaviors is found to be as narrow as 0.2 V. Refer to section 2-2, the standard deviation of devices from different glasses in mass production is 0.44V, which is larger than this boundary. This means if the TFTs are operated under this condition, the panel will exhibit serious and diverse degradation behavior and circuit performance may become unpredictable.

Chapter 4

Circuit performance of LTPS TFTs with device behavior variation

From the chapters above, it is demonstrated that LTPS TFTs suffer from serious variation and the variation of device behavior will diversify the reliability of LTPS TFTs under a critical stress condition. In this chapter, we use a commonly-used source follower configuration, which maybe the simplest function block, to examine the circuit performance affected by device variation.

4-1 Introduction to source follower

Source follower is often used as an output buffering circuit whose output load is connected in the source circuit of a field-effect transistor and whose input signal is applied between the gate and the remote end of the source load, which is usually at ground potential. This circuit is widely used in analog circuits because of its simplicity and low power consumption, which is required for nowaday displays. The simplest source follower configuration is shown in Fig.4-1, which is used in this work. The application and operation of a source follower are directly related to the threshold voltage (Vth) of the TFT. Typically, a source follower stops charging the load as the voltage drop between the gate Vg and source electrode Vs of the transistor is the threshold voltage of the transistor. It is expected that in the initial stage, the voltage difference between gate and source, Vgs, and between drain and source, Vds, are large and the charging of the capacitor is very fast. As time increases, the voltage difference Vgs and Vds both decrease and the charging behavior becomes slow. Conventionally, refer to Fig.4-2, when the source follower stops charging, the voltage of the load will be Vgs-Vth and the voltage difference between gate and source will be the Vth of the

transistor.

4-2 The charging behavior as the transistor is replaced

Fig.4-3 shows the drain current dependence on the gate voltage, namely the Id-Vg curves, of three typical LTPS TFTs. Based on the widely used extraction method, e.g., “Constant Current Method” which extracts threshold voltage at the gate voltage at the normalized current at Id/ (W/L) =10nA at drain voltage Vds=0.1 V, these three TFTs have similar value of threshold voltage. However, from Fig. 4-4, it can be seen that the output voltages do not stop at the voltage of Vgs-Vth around 3.5V, which is much different from our expectation. Furthermore, their output voltages show an unsaturated behavior. The reason the output voltages do not swiftly saturate is that LTPS TFTs have more gradual subthreshold transition behaviors than MOSFETs do[12~16]. As the source voltage increases and it is noticed that this special transition region is just where the typical constant current method designates. Thus, the concept of “threshold” for a LTPS TFT should be comprehended as a region instead of a specific point.

Since in source followers the voltage drop of gate to source (Vgs) and drain to source (Vds) keeps changing, it would be more appropriate to examine the current behavior with the changing Vs and fixed Vd and Vg. In Fig. 4-5, the characteristics of the TFTs are re-examined by their Id-Vs curves, which exhibit the dependence of Id on the source voltage Vs with Vg and Vd are kept constant. Comparing the source voltage in the Id-Vs curves and the voltage drop in the source follower charging curves, it depicts that the output voltage of the source follower is related to the current behavior of region B in the Id-Vs curves.

To verify the relation of the charging behavior and the device characteristics in region B, we modify the zerobias threshold voltage parameter Vto of the previous

three devices and name them as Device D, E and F, respectively. In Fig. 4-6 and Fig. 4-7, it can be seen that these devices have different threshold voltage and their Id-Vs curves coincide with the constant current at normalized drain current Id/(W/L)=10nA. As illustrated in Fig. 4-8, these devices have almost the same output voltage. Intuitively, devices having the same threshold voltage should have the same output voltage in the source follower. However, in LTPS TFT source followers, this nature is not observed. Besides, comparing Fig. 4-7 and Fig. 4-8, it is proposed that the Vth can be extracted by the voltage difference between the constant Vg and the Vs at the normalized current in the Id-Vs curves.

4-3 Discussion of the charging behavior and device variation

The reason source follower is chosen to examine the affected circuit performance is because of its simplicity. From the discussions above, it can be seen that as the transistor is replaced to the LTPS TFTs with similar threshold voltage and different subthreshold swing, the charging behavior and the output voltage are quite different from our expectation. It is attributed to the gradually-changing subthreshold current. This reveals that for source followers adopting LTPS TFTs, it will take two device parameters, the threshold voltage and the subthreshold swing, to characterize the source follower. Since there are serious variations in LTPS TFT device parameters, it can be predicted that the charging behavior of source followers will also result in serious variation. In an advanced circuitry, it can be inferred that circuit performance with more TFTs will be affected by the device variation more seriously. Therefore the variation issue of LTPS TFTs will be inevitable as the number of device increases and the circuit becomes complicated.

Chapter 5

Conclusion

In this thesis, we investigate the uniformity issue of LTPS TFTs. Firstly we aim at the nature of device variation. We classify the variation as macro variation and micro variation. Since device parameters from different glasses are actually mixing up macro variation and micro variation, we further use the "crosstie" layout to banish macro variation from micro variation. By analyzing the variance of electrical behavior with respect to difference device interval, we confirm that the main source of variation for the neighboring devices comes from the micro variation. As the device distance increases, macro variation will gradually become serious and it is found that as the device distance increases to 2 cm, the effect of macro variation will become apparent. By introducing a statistical formula, it is further found that micro variation does not change as device distance increases.

Next we objectively demonstrated the difficulties in analyzing device reliability and circuit performance affected by device behavior variation. Conventionally, devices under the same stress condition should exhibit similar degradation behavior. However, in our experiment, it is found that the devices with different threshold voltage will exhibit different degradation behavior under the same stress condition. It is also found that there seems a boundary separating these two degradation mechanism by the value (Vg,str-Vt). Devices with different threshold voltage will exhibit diverging degradation behavior under this stress condition. It can consequently be inferred that the reliability prediction would be affected by device variation.

For circuit performance, we use a simple component to examine the influence from device variation. Source follower is chosen not only because of its wide usage but of its simplicity. As the transistor is replaced to the LTPS TFTs with similar

threshold voltage and different subthreshold swing, the charging behavior and the output voltage are quite different from our expectation. The output voltage exhibits the unsaturated behavior and is directly affected by the variation of device parameter. Since source follower may be the simplest circuit, we could infer that the variation issue of the devices may lead to worse performance and more difficult to predict the behavior of more advanced circuitry with LTPS TFTs.

From the viewpoints of circuit and device performance, the variation of device behavior will lead to extra difficulties in prediction. Hence it will be crucial to get a better understanding of the source of device variation. In our work, we have classified and quantitatively distinguished macro and micro variation. However, before LTPS TFTs can be widely adopted in flat panel display, the variation behavior of LTPS TFTs should be further investigated.

References

[1] S. Inoue, M. Kimura and T. Shimoda, SID ’00 Dig., 2000, p. 365.

[2] S. Inoue and T. Shimoda: SID ’99 Dig., 1999, p. 452.

[3] Y. Uraoka, N. Hirai, H. Yano, T. Hatayama, and T. Fuyuki, IEEE ELECTRON DEVICE LETTERS, VOL. 24, NO. 4, APRIL 2003, p.236

[4] Y. Uraoka, T. Hatayama, T. Fuyuki, T. Kawamura and Y. Tsuchihashi, Jpn. J. Appl. Phys. 39 (2000) L1209.

[5] T. Sameshima, Y. Sunaga and A. Kohno, Jpn. J. Appl. Phys. 35 (1996) L308.

[6] N. Kato, T. Yamada, S. Yamada, T. Nakamura and T. Hamano, IEDM Tech. Dig., 1992, p. 677.

[7] K. Okuyama, K. Kubota, T. Hashimoto, S. Ikeda and A. Koike: IEDM Tech. Dig., 1993, p. 527.

[8] S. Inoue, M. Kimura and T.Shimoda, Jpn. J. Appl. Phys. Vol. 42 (2003) pp. 1168–1172

[9] S. Inoue, S. Takenaka and T. Shimoda, Jpn. J. Appl. Phys. Vol. 42 (2003) pp. 4213–4217

[10] K. C. Lin, C.W. Hu and C.W. Cheng, IDMC '05 p. 438-441

[11] S. Inoue, M. Kimura and T.Shimoda, Jpn. J. Appl. Phys. Vol. 41 (2002) pp. 6313–6319

[12] Mark D.Jacunski, Michael Shur, Michael Hack, IEEE Transactions on Electron Devices, Vol.43, No.9 (1996)

[13] B.Iniguez, Z.Xu, T.Fjeldly and M.S.Shur Proc.IEEE 1999 Int. Conf. on Microelectronic Test Structures, Vol 12, (1999)

[14] Jacunski, Mark D.; Shur, Michael S.; Hack, Michael, IEEE Transactions on Electron Devices, v 43, n 9, Sep, p 1433-1440 (1996)

[15] Peyman Servati, Denis Striakhilev, Arokia Nathan, IEEE Transactions on Electron Devices, VOL. 50, NO. 11,(2003)

[16] A. Ortiz-Conde, F.J. Garcia Sanchez, J.J. Liou, A Cerdeira, M. Estrada, Y. Yue, Microelectronics Reliability, Vol.42, p.583-596 (2002)

Figure caption- Chapter 2

Fig 2-2-1 The mean value and deviation of threshold voltage of different sites.
Fig 2-2-2 The mean value and deviation of mobility of different sites.
Fig 2-2-3 The mean value and deviation of subthreshold swing of different sites.
Fig 2-2-4 The relative position of the eight sites discussed in section 2-2.
Fig 2-3-1 The crosstie type layout of LTPS TFTs.
Fig 2-3-2 The histogram of Vth of horizontal crosstie devices.
Fig 2-3-3 The Q-Q plot of Vth of horizontal crosstie devices.
Fig 2-3-4 The detrended Q-Q plot of Vth of horizontal crosstie devices.
Fig 2-3-5 The histogram of mobility of horizontal crosstie devices.
Fig 2-3-6 The Q-Q plot of mobility of horizontal crosstie devices.
Fig 2-3-7 The detrended Q-Q plot of mobility of horizontal crosstie devices.
Fig 2-3-8 The histogram of subthreshold swing of horizontal crosstie devices.
Fig 2-3-9 The Q-Q plot of subthreshold swing of horizontal crosstie devices.
Fig 2-3-10 The detrended Q-Q plot of subthreshold swing of horizontal crosstie devices.
Fig 2-3-11 The histogram of Vth difference of device step 1 horizontally
Fig 2-3-12 The histogram of Vth difference of device step 12 horizontally
Fig 2-3-13 The histogram of Vth difference of device step 36 horizontally
Fig 2-3-14 The histogram of Vth difference of device step 120 horizontally
Fig 2-3-15 The histogram of Vth difference of device step 1340 horizontally
Fig 2-3-16 The histogram of Vth difference of device step 1380 horizontally
Fig 2-3-17 The histogram of Vth difference of device step 1460 horizontally
Fig 2-3-18 The threshold voltage of the crosstie devices on different position
Fig 2-3-19 The average and deviation value of the Vth difference of the crosstie devices with different device distance

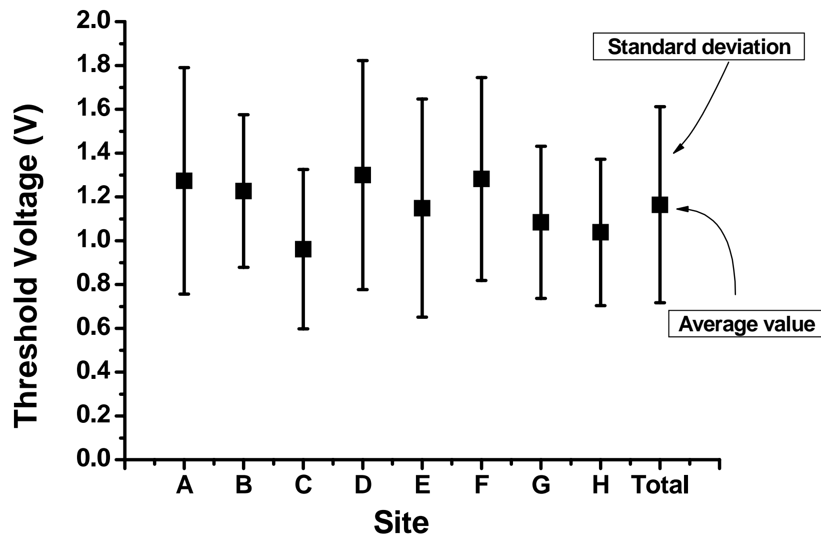

Fig 2-2-1　The mean value and deviation of threshold voltage of different sites.

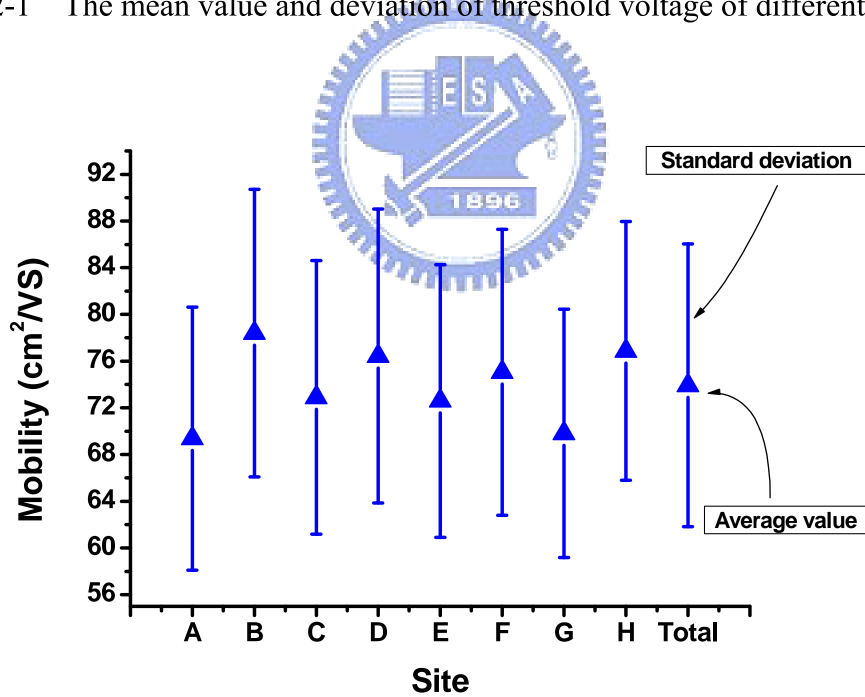

Fig 2-2-2　The mean value and deviation of mobility of different sites.

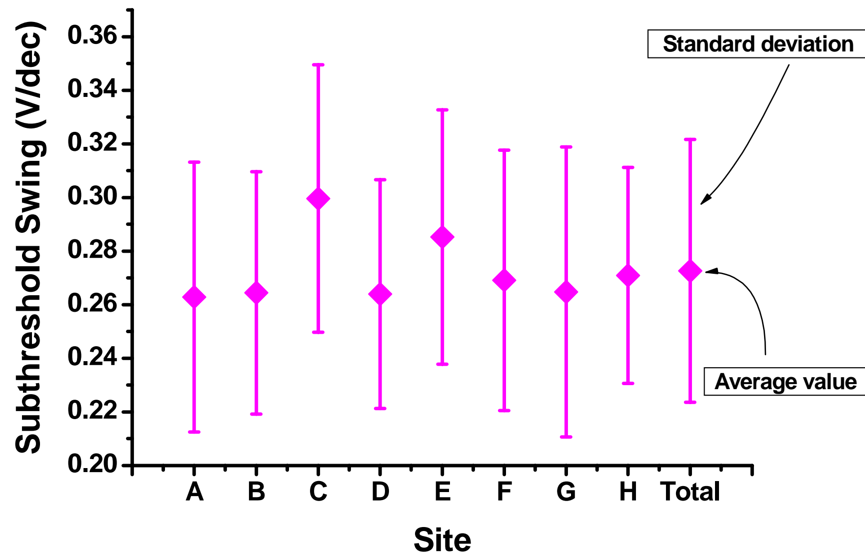

Fig 2-2-3 The mean value and deviation of subthreshold swing of different sites.

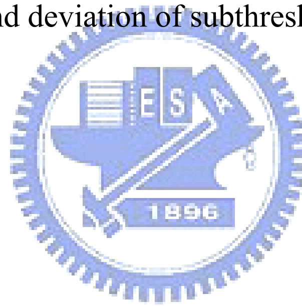

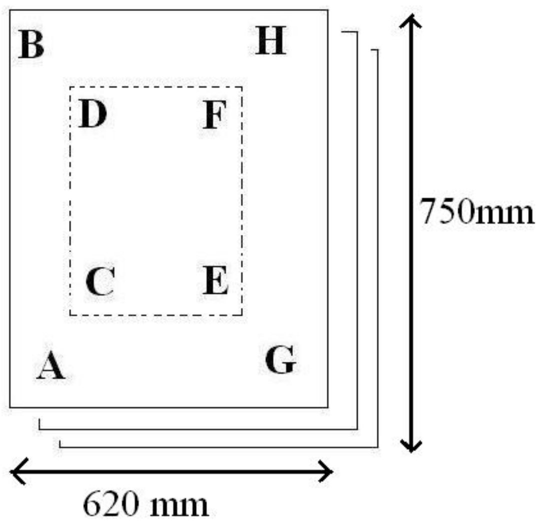

Fig 2-2-4 The relative position of the eight sites discussed in section 2-2.

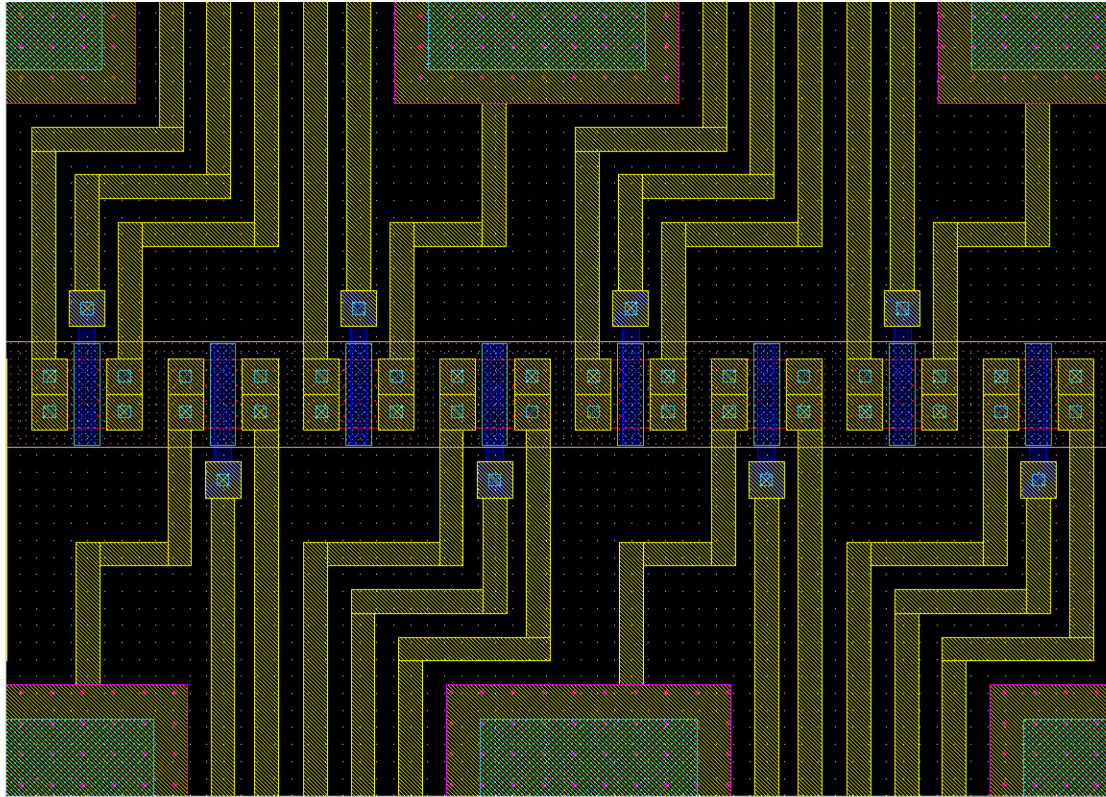

Fig 2-3-1 The crosstie type layout of LTPS TFTs.

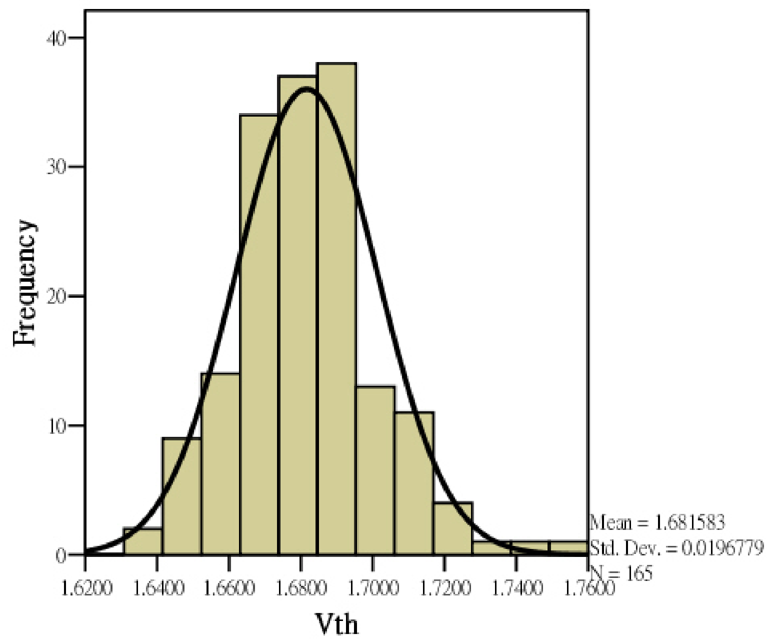

Fig 2-3-2 The histogram of Vth of horizontal crosstie devices.

Normal Q-Q Plot of Vth of horizontal devices

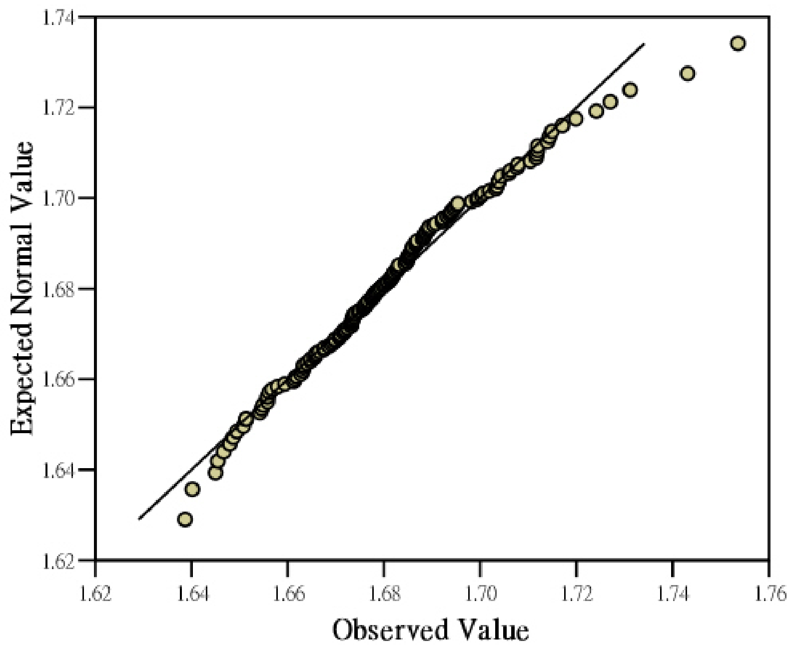

Fig 2-3-3 The Q-Q plot of Vth of horizontal crosstie devices.

Detrended Normal Q-Q Plot of Vth of horizontal devices

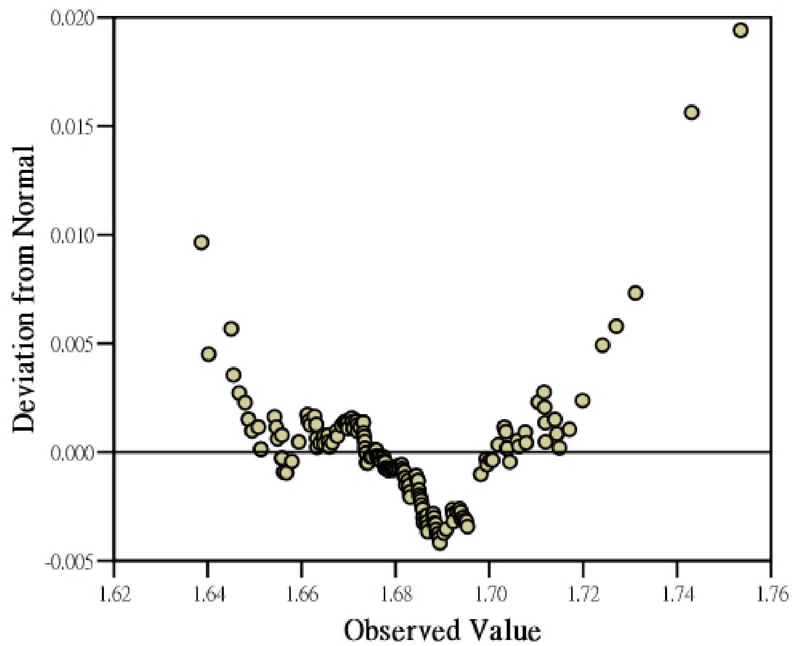

Fig 2-3-4 The detrended Q-Q plot of Vth of horizontal crosstie devices.

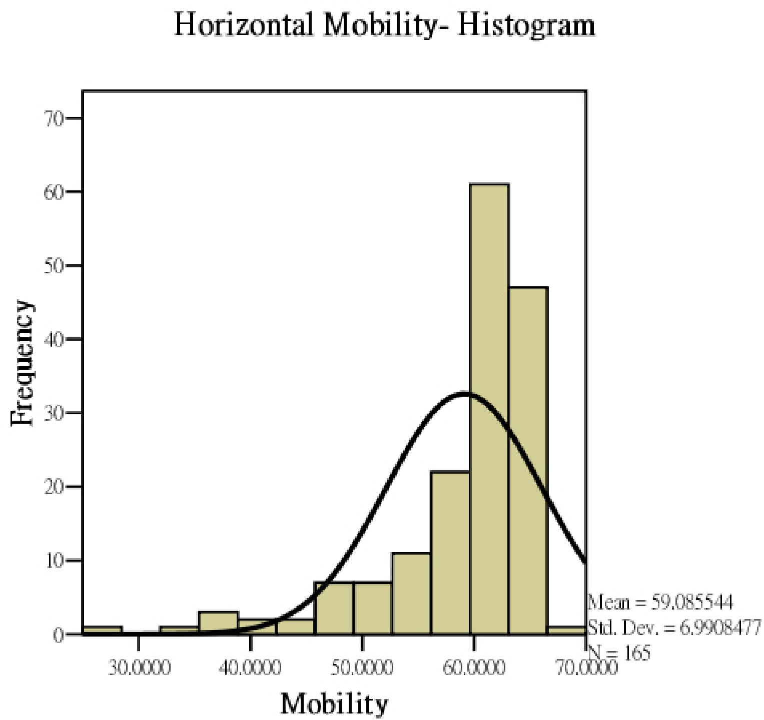

Fig 2-3-5 The histogram of mobility of horizontal crosstie devices.

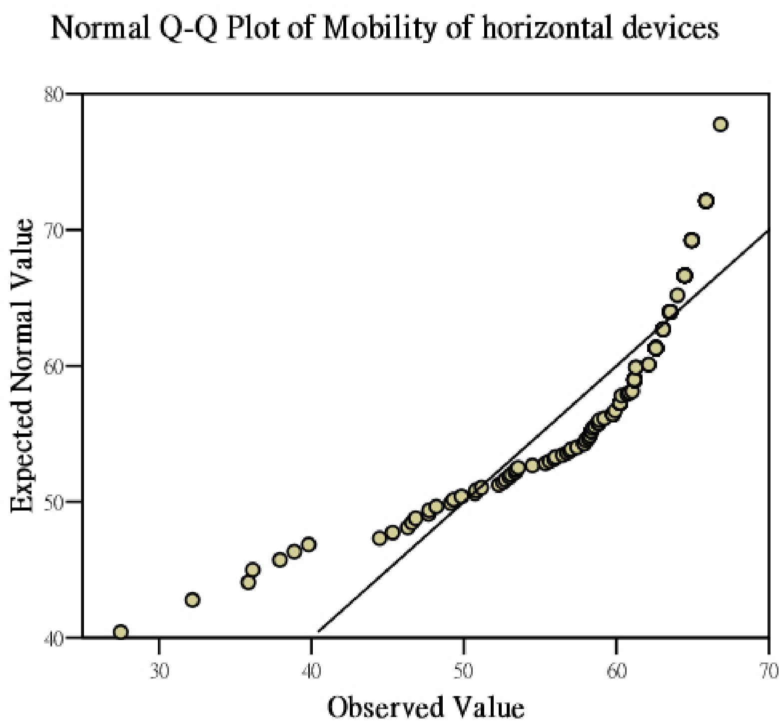

Fig 2-3-6 The Q-Q plot of mobility of horizontal crosstie devices.

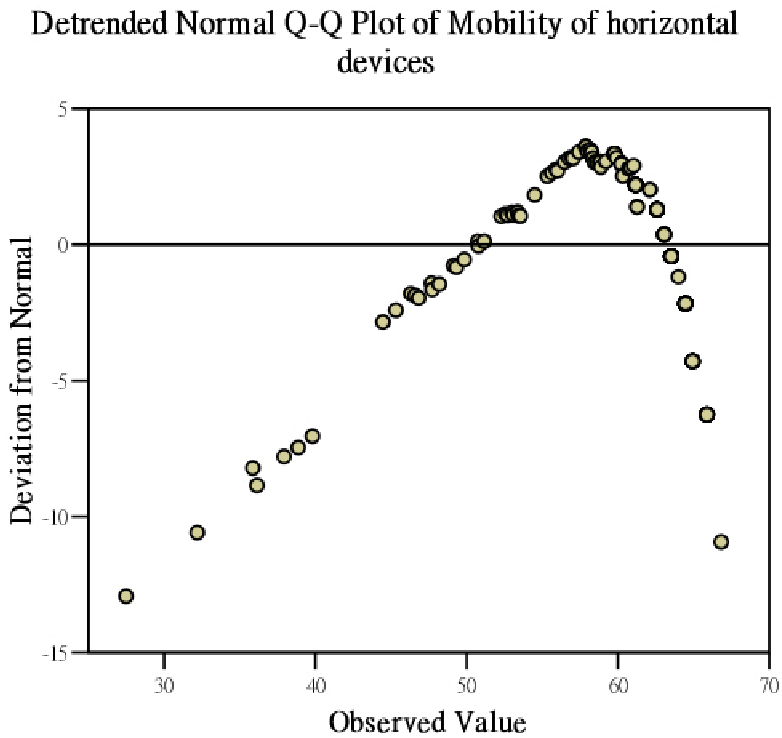

Fig 2-3-7 The detrended Q-Q plot of mobility of horizontal crosstie devices.

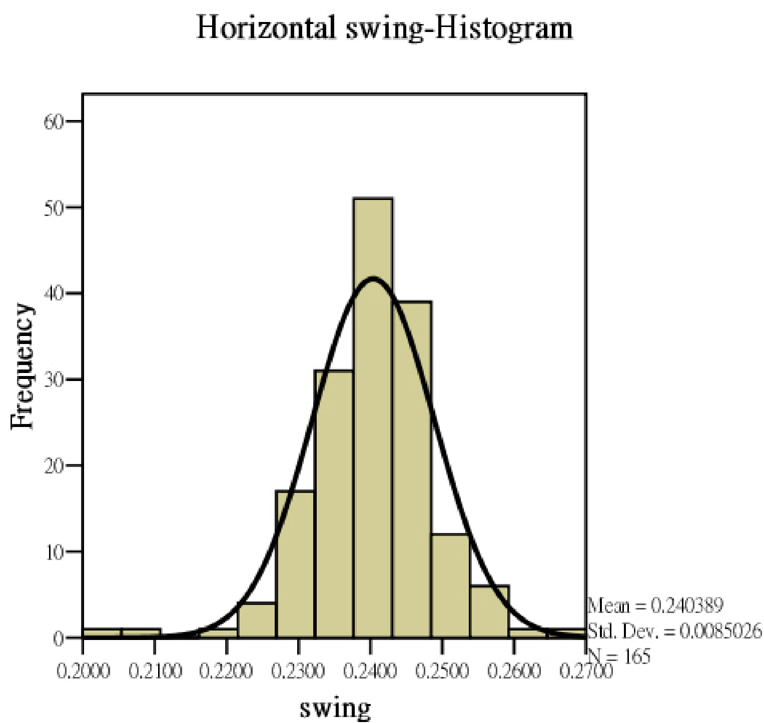

Fig 2-3-8 The histogram of subthreshold swing of horizontal crosstie devices.

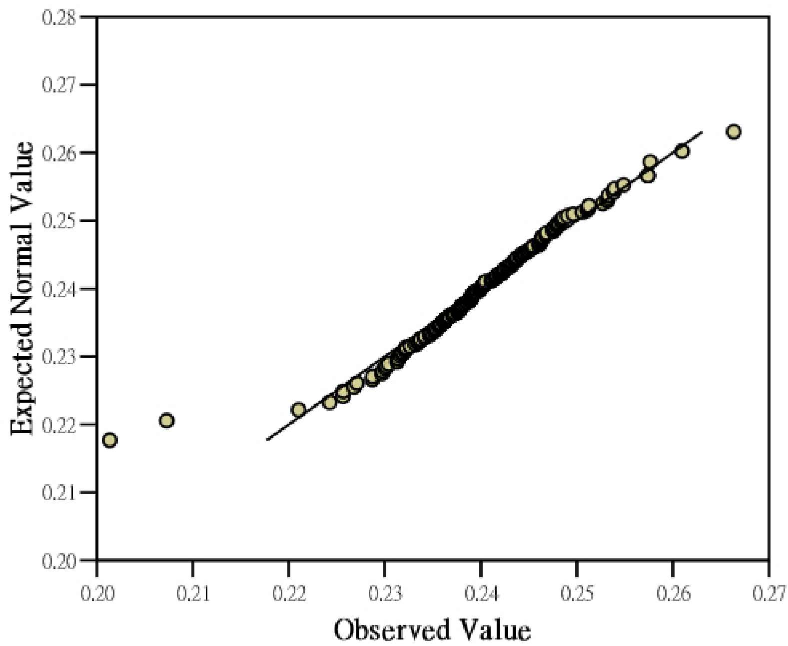

Fig 2-3-9　The Q-Q plot of subthreshold swing of horizontal crosstie devices.

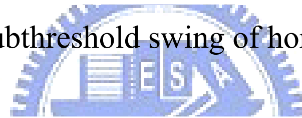

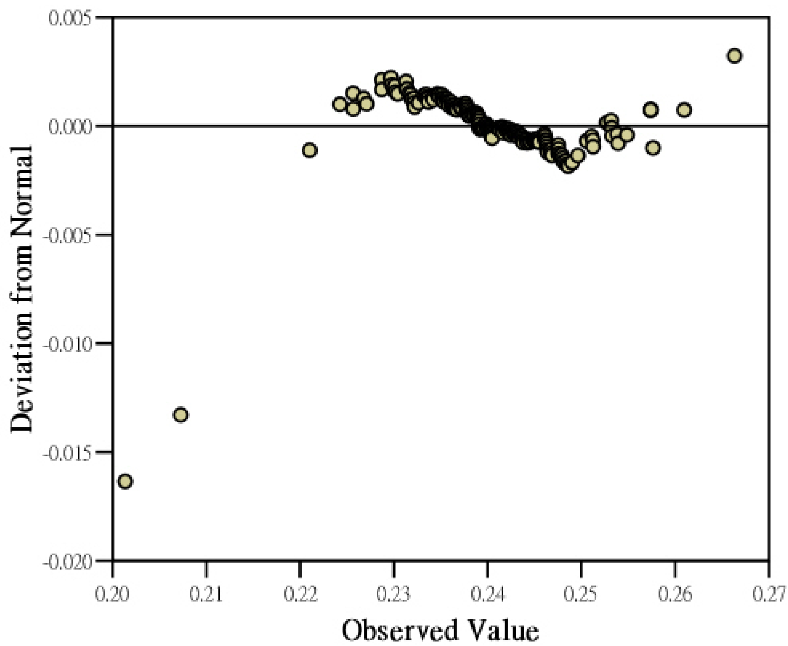

Fig 2-3-10　The detrended Q-Q plot of subthreshold swing of horizontal crosstie devices.

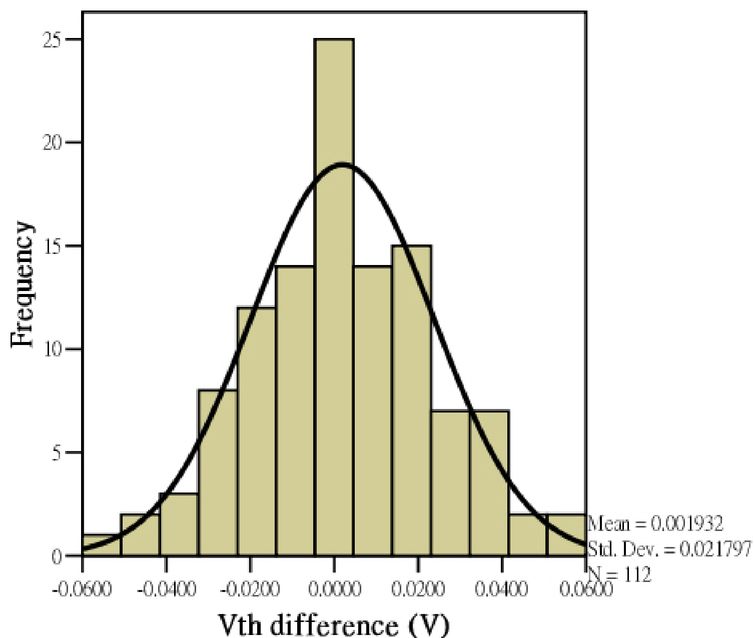

Fig 2-3-11 The histogram of Vth difference of device step 1 horizontally

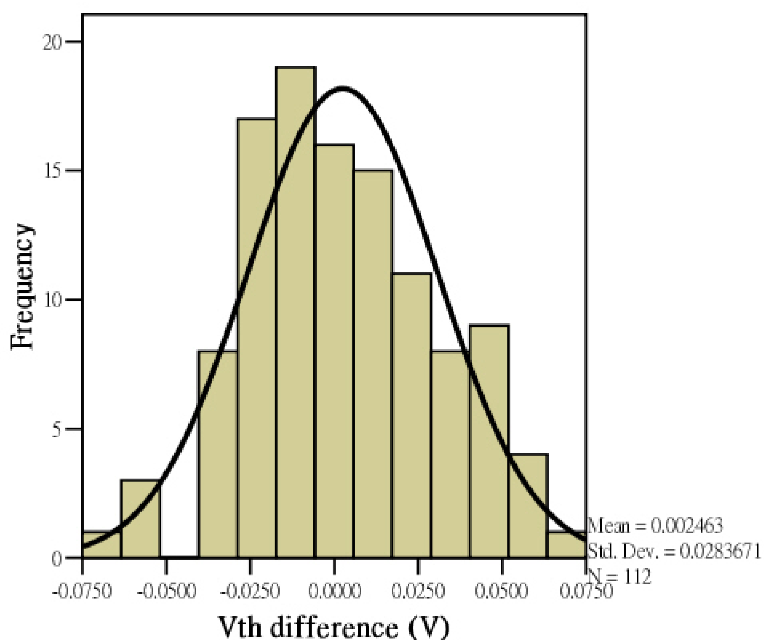

Fig 2-3-12 The histogram of Vth difference of device step 12 horizontally

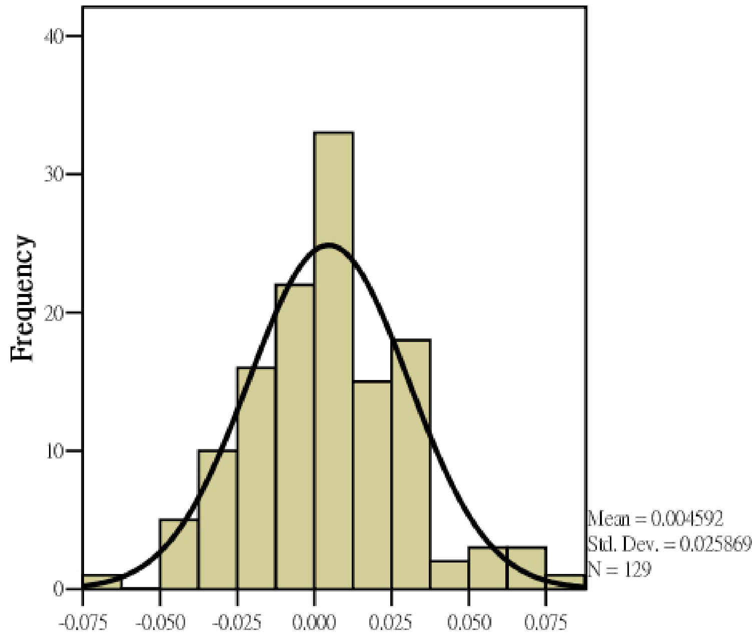

Fig 2-3-13 The histogram of Vth difference of device step 36 horizontally

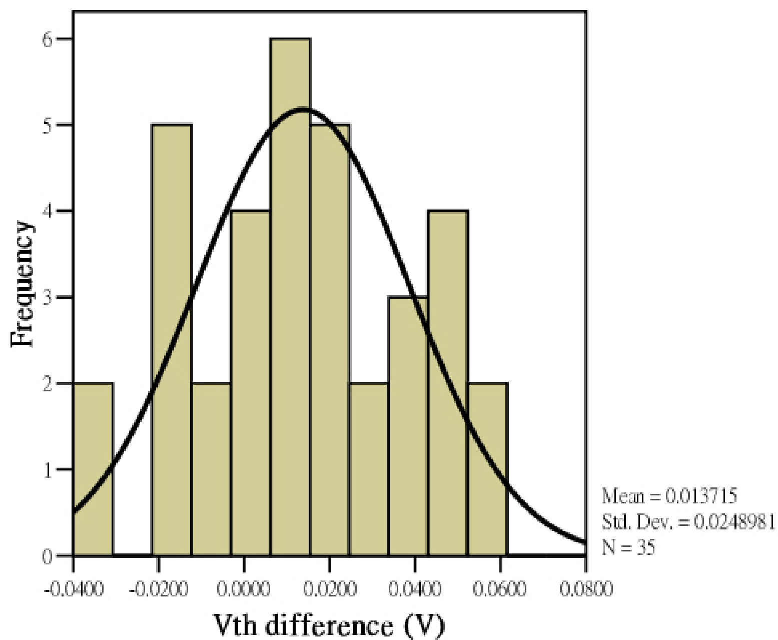

Fig 2-3-14 The histogram of Vth difference of device step 120 horizontally

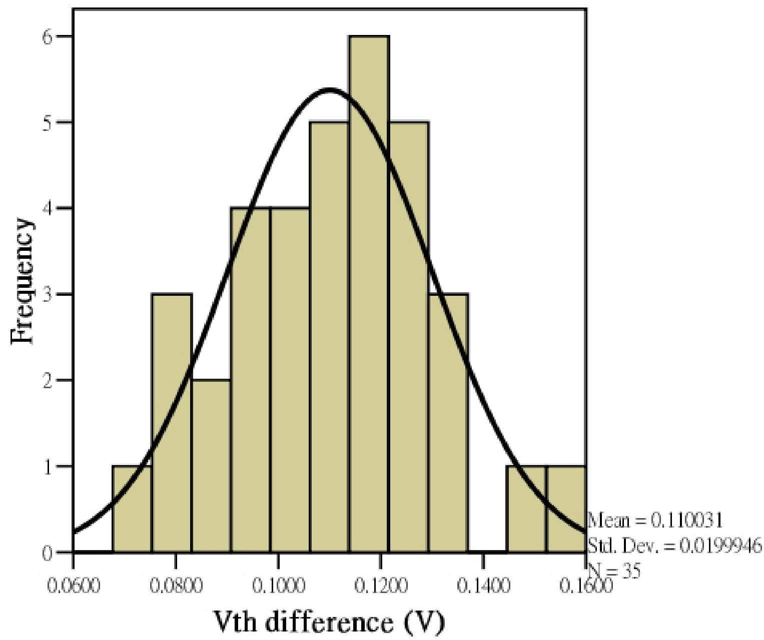

Fig 2-3-15 The histogram of Vth difference of device step 1340 horizontally

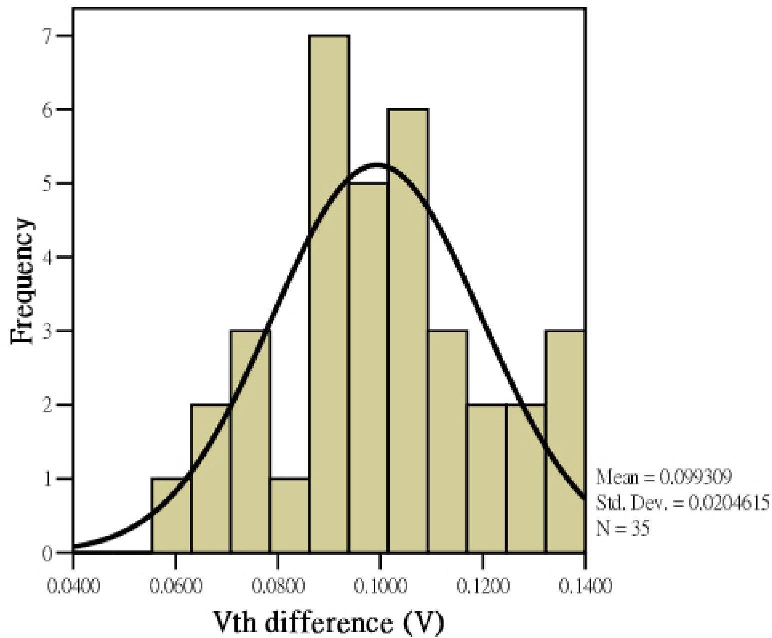

Fig 2-3-16 The histogram of Vth difference of device step 1380 horizontally

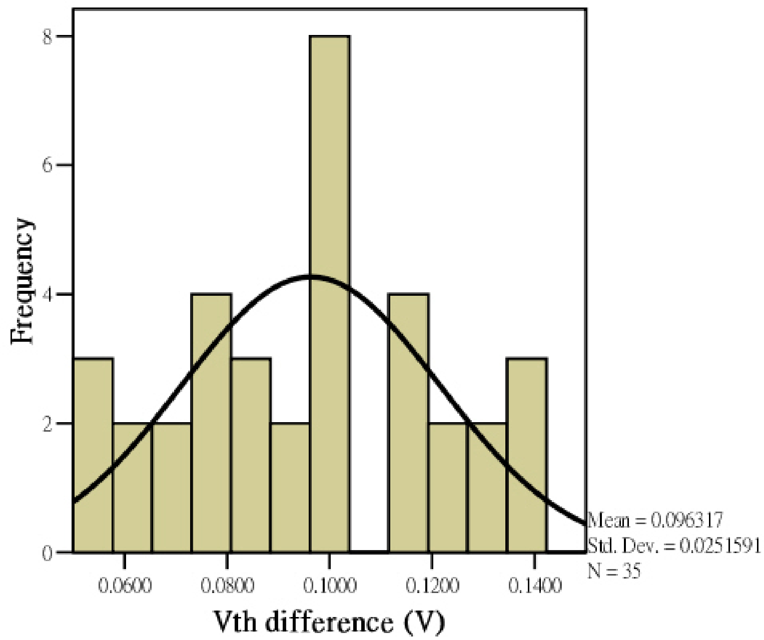

Fig 2-3-17 The histogram of Vth difference of device step 1460 horizontally

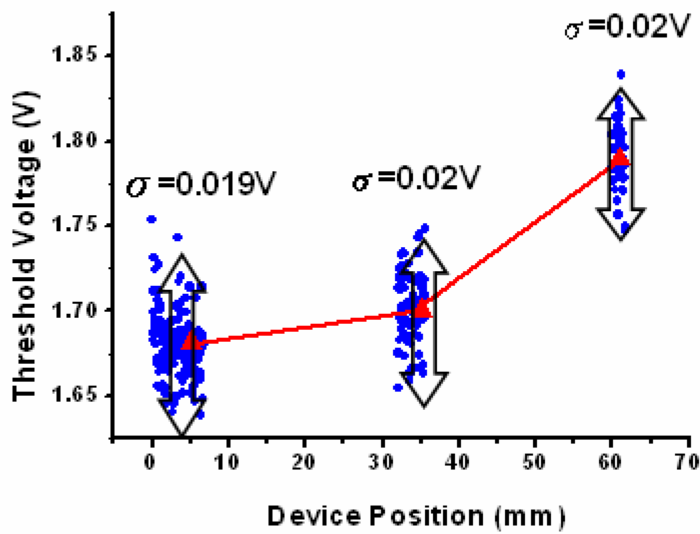

Fig 2-3-18 The threshold voltage of the crosstie devices on different position

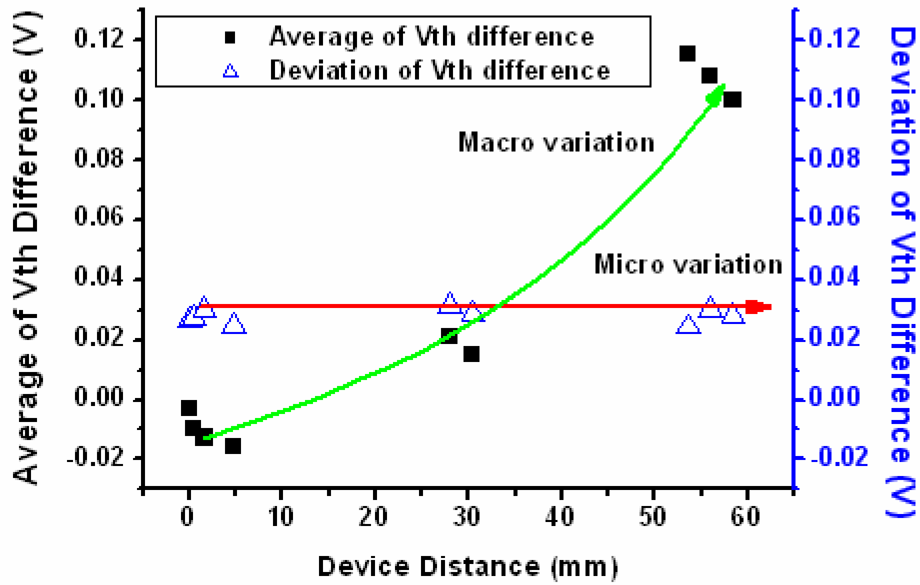

Fig 2-3-19 The average and deviation value of the Vth difference of the crosstie devices with different device distance

Figure caption- Chapter 3

Fig. 3-2-1 The transfer characteristics and degradation behavior of the LTPS TFTs under stress conditions for thermal effect.

Fig. 3-2-2 The transfer characteristics and degradation behavior of the LTPS TFTs under stress conditions for hot carrier effect.

Fig. 3-2-3 The swing degradation of devices with respect to different stress gate voltage and drain voltage is kept at 20V.

Fig. 3-2-4 The swing degradation with respect to stress gate voltage (Vg,stress) (solid dots) and the difference between stress gate voltage and initial threshold voltage (Vg,stress-Vt) (empty dots).

Fig. 3-2-5 The degradation in the transfer curves of the device A and B with smaller Vth.

Fig. 3-2-6 The degradation in the transfer curves of the device X and Y with larger Vth.

Fig. 3-2-7 The degradation in the transfer curves of the device D with intermediate Vth.

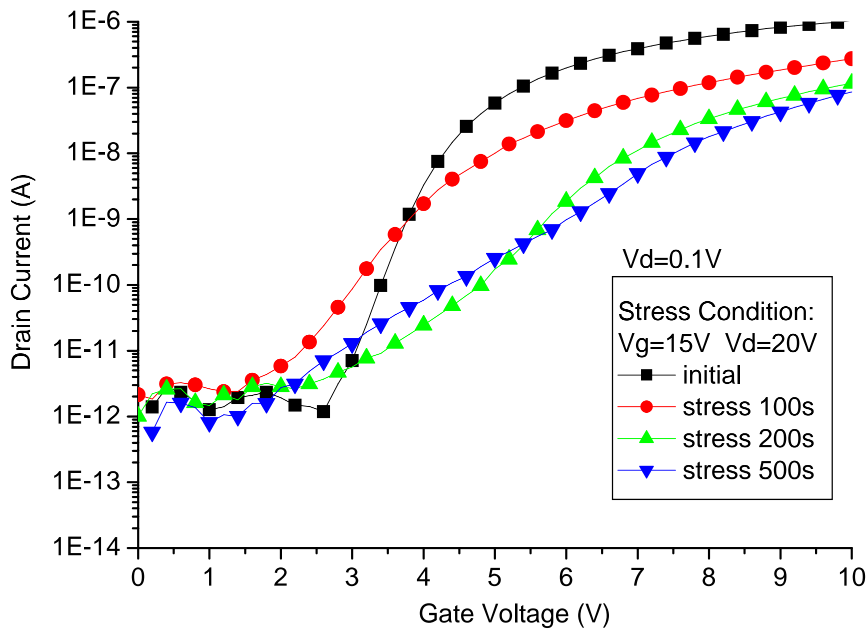

Fig. 3-2-1 The transfer characteristics and degradation behavior of the LTPS TFTs under stress conditions for thermal effect.

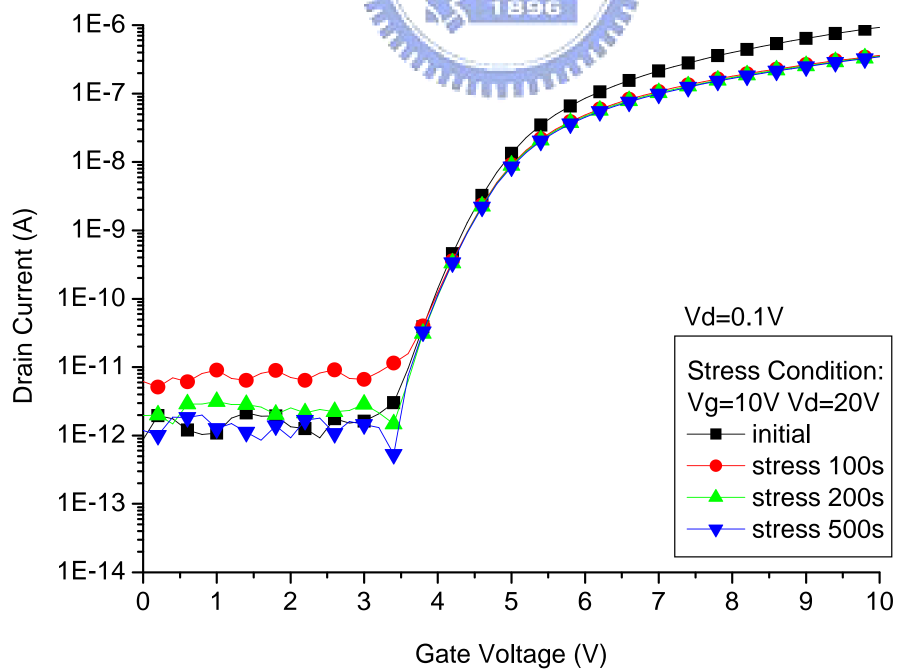

Fig. 3-2-2 The transfer characteristics and degradation behavior of the LTPS TFTs under stress conditions for hot carrier effect.

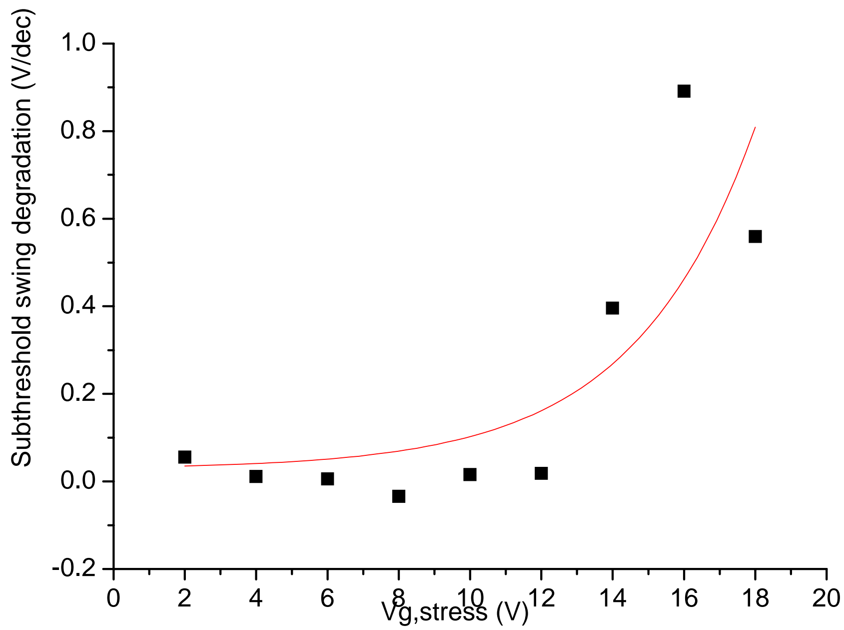

Fig. 3-2-3 The swing degradation of devices with respect to different stress gate voltage and drain voltage is kept at 20V.

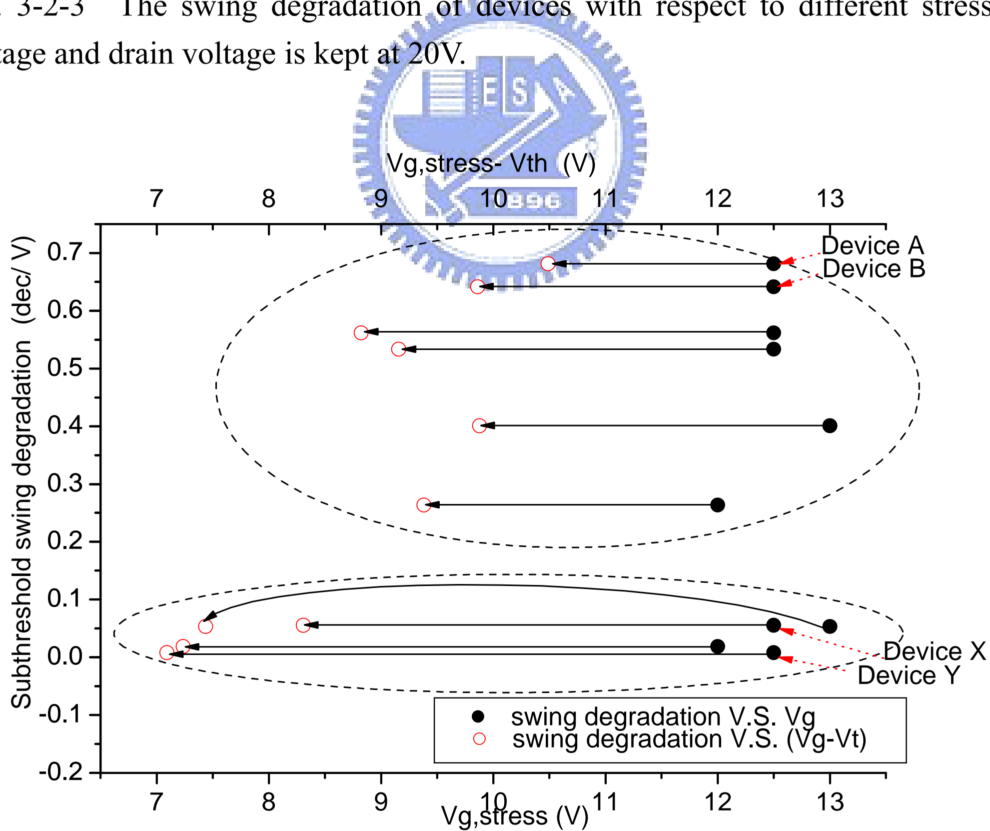

Fig. 3-2-4 The swing degradation with respect to stress gate voltage (Vg,stress) (solid dots) and the difference between stress gate voltage and initial threshold voltage (Vg,stress-Vt) (empty dots).

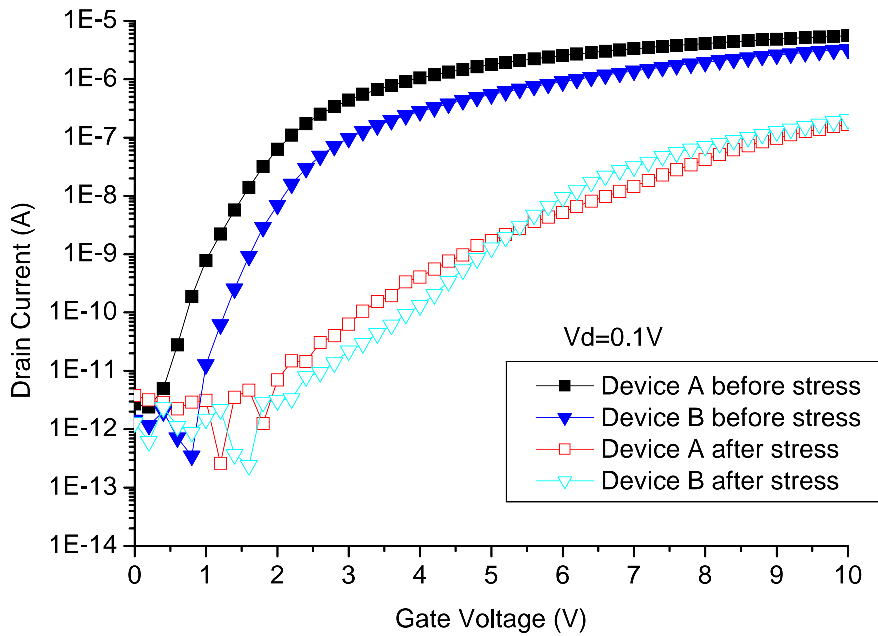

Fig. 3-2-5 The degradation in the transfer curves of the device A and B with smaller Vth.

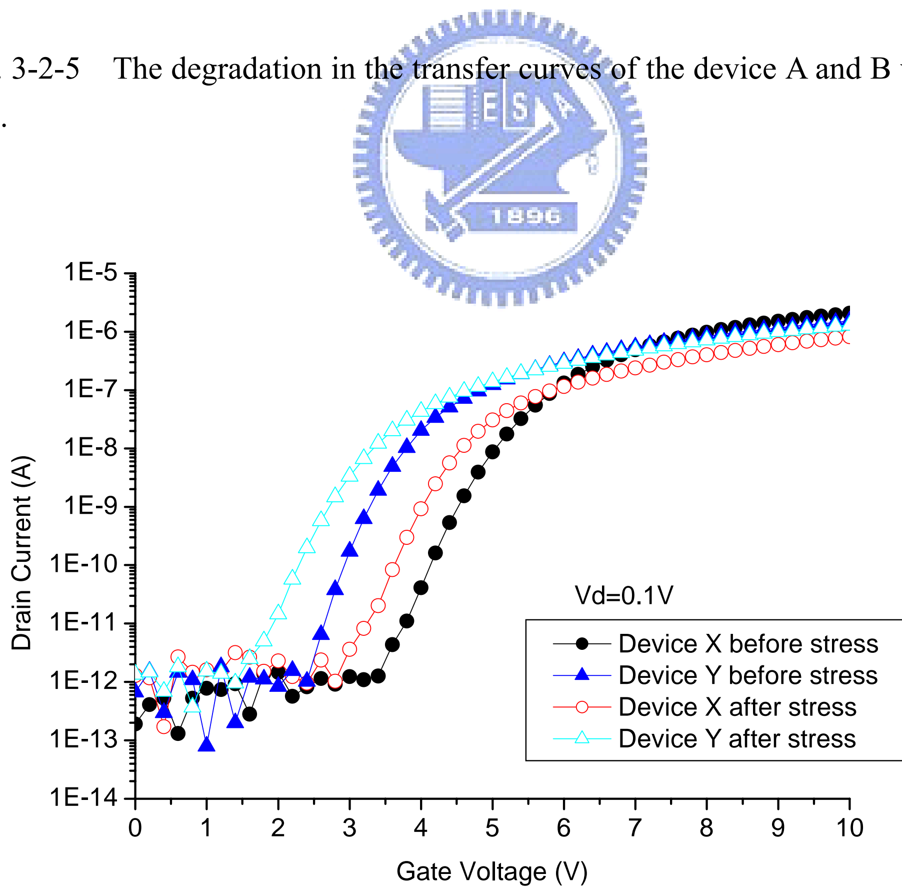

Fig. 3-2-6 The degradation in the transfer curves of the device X and Y with larger Vth.

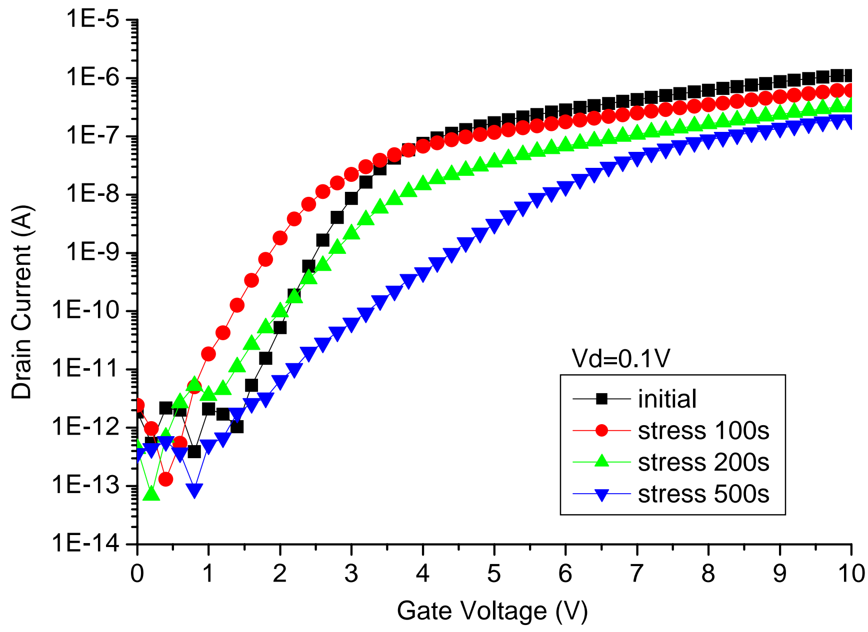

Fig. 3-2-7 The degradation in the transfer curves of the device D with intermediate Vth.

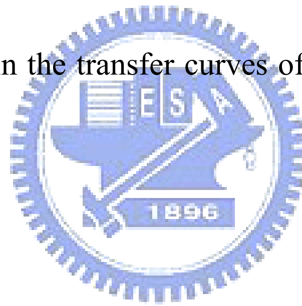

Figure Caption – Chapter 4

Fig. 4-1. The source follower configuration used in this work.
Fig. 4-2. The typical chaging behavior of the source follower.
Fig. 4-3. The Id-Vgs of the three poly-Si TFT curves with the similar threshold voltage.
Fig. 4-4. The charging behavior of the source followers using the three TFTs.
Fig. 4-5. The Id-Vs curves of the device A, B, and C which have similar Vth value from the typical extraction method.
Fig. 4-6. The Id-Vg curve of the other three devices. They have different Vth.
Fig. 4-7. The Id-Vs curves of the the device D,E and F.
Fig. 4-8. The charging curves of the source follower for three TFTs corresponding to Fig 4-7.

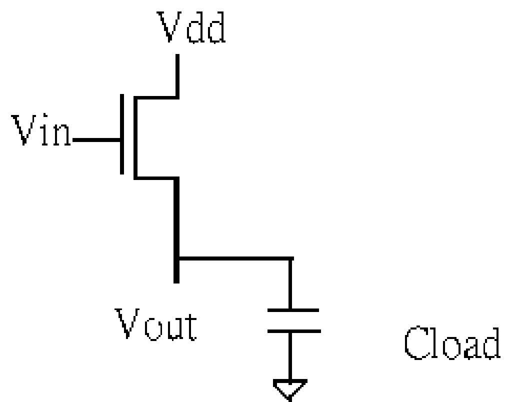

Fig. 4-1　The source follower configuration used in this work.

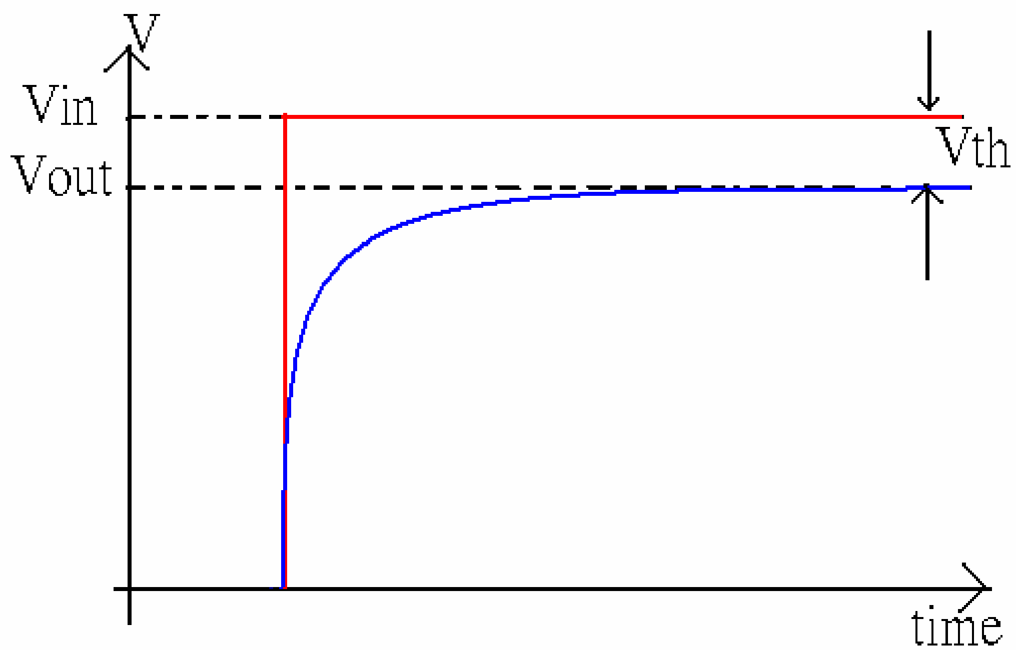

Fig. 4-2　The typical chaging behavior of the source follower.

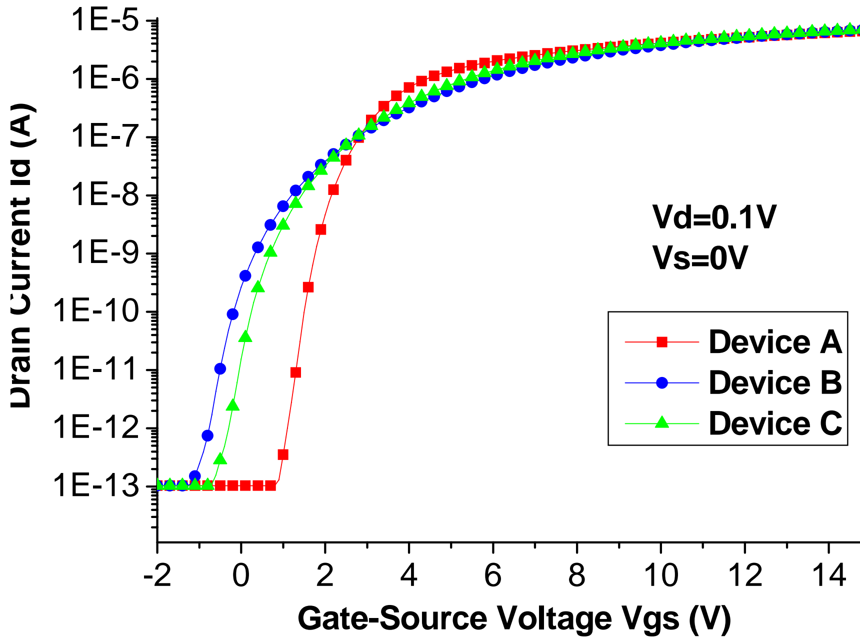

Fig. 4-3 The Id-Vgs of the three poly-Si TFT curves with the similar threshold voltage.

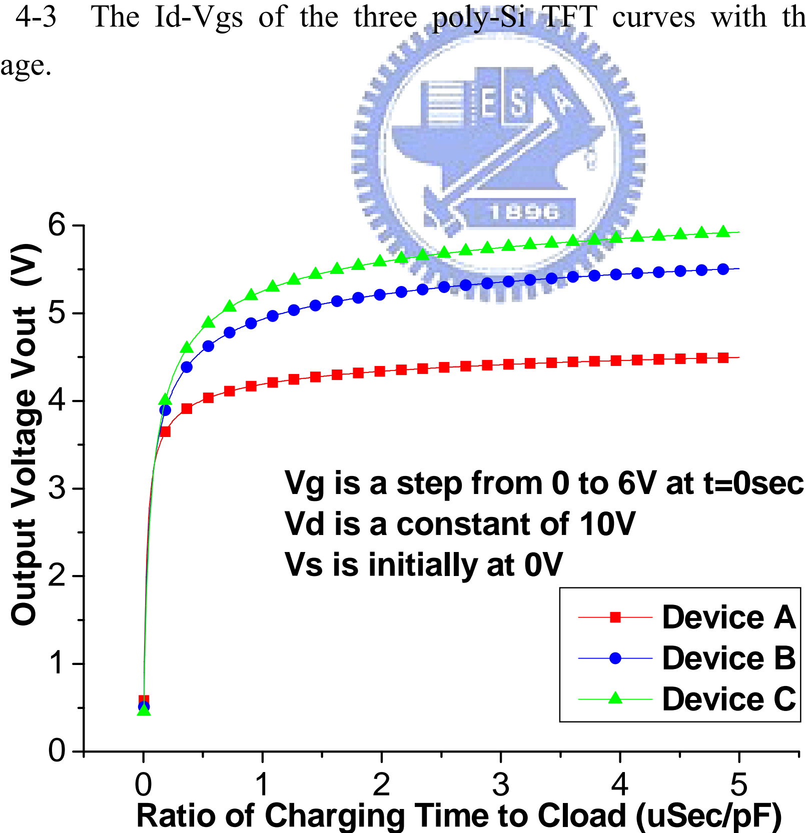

Fig. 4-4 The charging behavior of the source followers using the three TFTs.

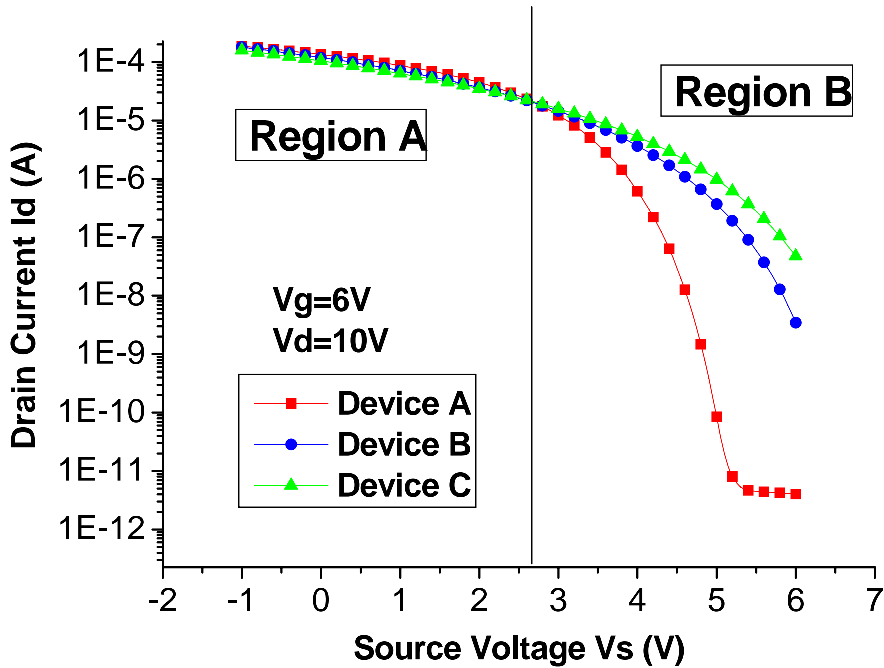

Fig. 4-5 The Id-Vs curves of the device A, B, and C which have similar Vth value from the typical extraction method.

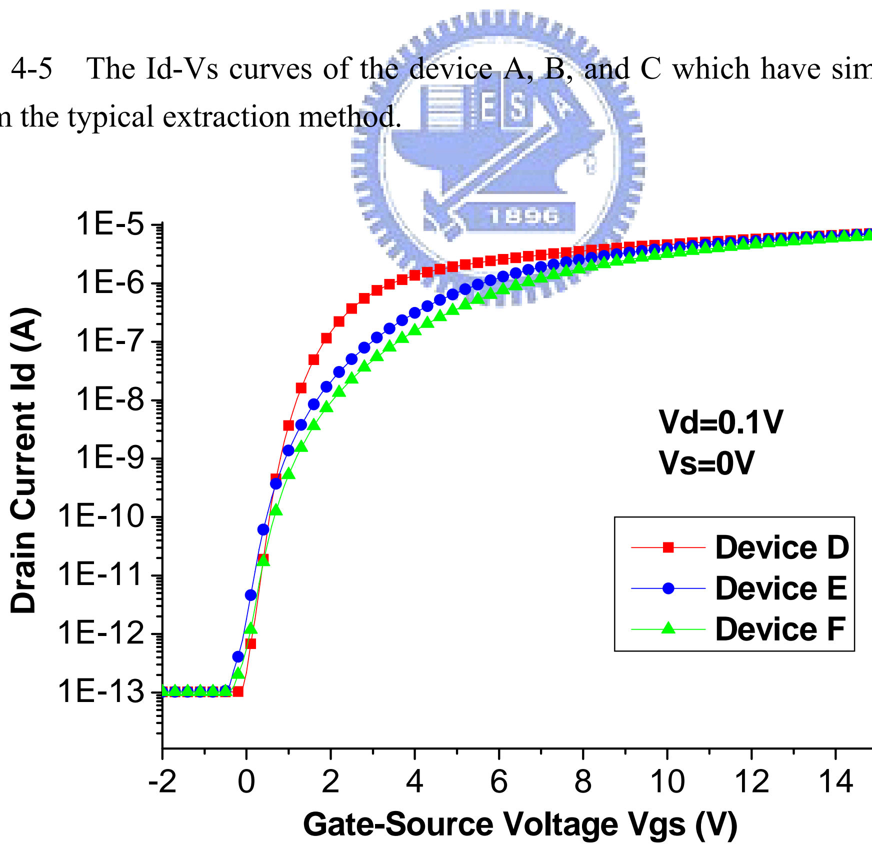

Fig. 4-6 The Id-Vg curve of the other three devices. They have different Vth.

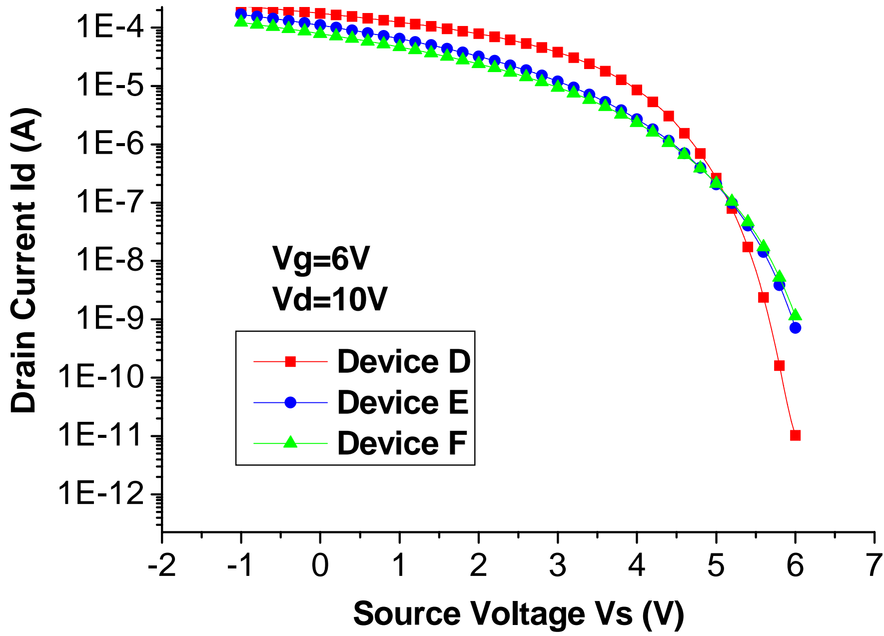

Fig. 4-7 The Id-Vs curves of the the device D,E and F.

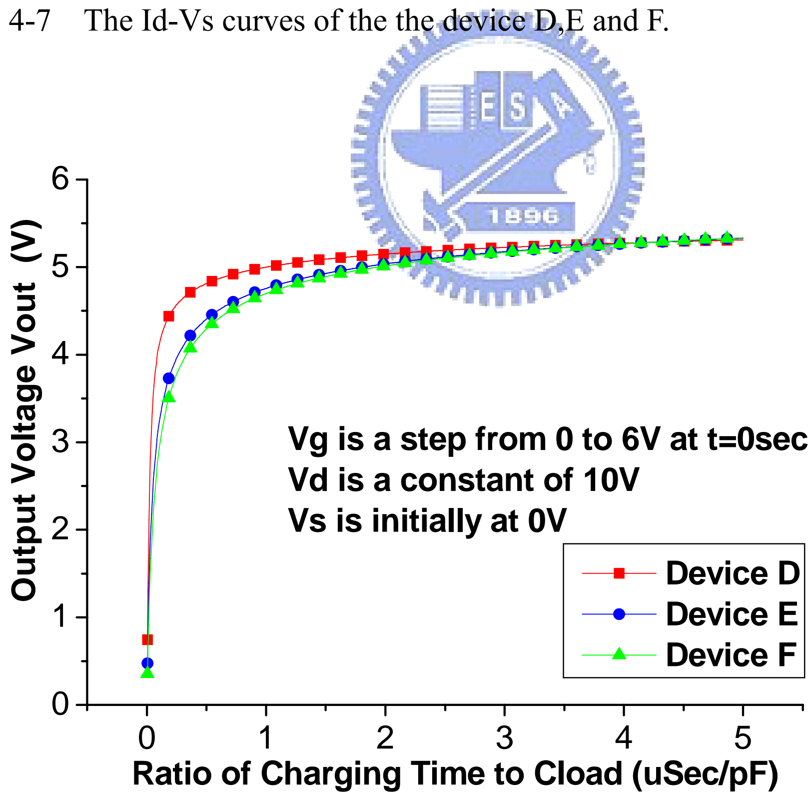

Fig. 4-8 The charging curves of the source follower for three TFTs corresponding to Fig 4-7.